FEBS Letters 583 (2009) 787–791

ELSEVIER

FEBS Letters

journal homepage: www.FEBSLetters.org

Inhibition of α-synuclein fibril assembly by small molecules: Analysis using epitope-specific antibodies

Masami Masuda [a,b], Masato Hasegawa [a,*], Takashi Nonaka [a], Takayuki Oikawa [a,b], Motokuni Yonetani [a,b], Yoshiki Yamaguchi [c], Koichi Kato [c], Shin-ichi Hisanaga [b], Michel Goedert [d,*]

[a] *Department of Molecular Neurobiology, Tokyo Institute of Psychiatry, 2-1-8 Kamikitazawa, Setagaya-ku, Tokyo 156-8585, Japan*
[b] *Molecular Neuroscience Laboratory, Graduate School of Science, Tokyo Metropolitan University, 1-1 Minami-Osawa, Hachioji-shi Tokyo 192-0397, Japan*
[c] *Department of Structural Biology and Biomolecular Engineering, Graduate School of Pharmaceutical Science, Nagoya City University, 3-1 Tanabe-dori, Mizuho-ku, Nagoya 467-8603, Japan*
[d] *MRC Laboratory of Molecular Biology, Hills Road, Cambridge CB2 0QH, UK*

FEBS Letters 583 (2009) 787–791

ELSEVIER

FEBS Letters

journal homepage: www.FEBSLetters.org

Inhibition of α-synuclein fibril assembly by small molecules: Analysis using epitope-specific antibodies

Masami Masuda [a,b], Masato Hasegawa [a,*], Takashi Nonaka [a], Takayuki Oikawa [a,b], Motokuni Yonetani [a,b], Yoshiki Yamaguchi [c], Koichi Kato [c], Shin-ichi Hisanaga [b], Michel Goedert [d,*]

[a] Department of Molecular Neurobiology, Tokyo Institute of Psychiatry, 2-1-8 Kamikitazawa, Setagaya-ku, Tokyo 156-8585, Japan
[b] Molecular Neuroscience Laboratory, Graduate School of Science, Tokyo Metropolitan University, 1-1 Minami-Osawa, Hachioji-shi Tokyo 192-0397, Japan
[c] Department of Structural Biology and Biomolecular Engineering, Graduate School of Pharmaceutical Science, Nagoya City University, 3-1 Tanabe-dori, Mizuho-ku, Nagoya 467-8603, Japan
[d] MRC Laboratory of Molecular Biology, Hills Road, Cambridge CB2 0QH, UK

ARTICLE INFO

Article history:
Received 8 December 2008
Revised 3 January 2009
Accepted 20 January 2009
Available online 4 February 2009

Edited by Jesus Avila

Keywords:
Tau
Amyloid
Polyphenol
Oligomer
Conformation
Aggregation

ABSTRACT

The conversion of soluble peptides and proteins into amyloid fibrils and/or intermediate oligomers is believed to be the central event in the pathogenesis of most human neurodegenerative diseases. Existing treatments are at best symptomatic. Accordingly, small molecule inhibitors of amyloid fibril formation and their mechanisms are of great interest. Here we report that the conformational changes undergone by α -synuclein as it assembles into amyloid fibrils can be detected by epitope-specific antibodies. We show that the conformations of polyphenol-bound α-synuclein monomers and dimers differ from those of unbound monomers and resemble amyloid fibrils. This strongly suggests that small molecule inhibitors bind and stabilize intermediates of amyloid fibril formation, consistent with the view that inhibitor-bound molecular species are on-pathway intermediates.

1. Introduction

The conversion of a small number of soluble peptides and proteins into amyloid fibrils and/or intermediate oligomers is believed to be the central event in the pathogenesis of most neurodegenerative diseases. Three proteins, β-amyloid, tau and α-synuclein, make up the abnormal deposits in the vast majority of disease cases [1,2]. Many current therapeutic strategies are aimed at inhibiting filament formation and at promoting filament clearance. In recent years, a number of compounds has been identified that prevent amyloid fibril formation in vitro [3–10]. In the absence of effective therapies for neurodegenerative diseases, it is important to understand the mechanisms of action of these compounds.

We previously reported that non-toxic, SDS-stable dimers and oligomers of tau and α-synuclein formed in the presence of inhibitory compounds and that their formation closely correlated with the inhibition of fibril formation [8,9]. This suggests that small molecule inhibitors stabilize non-toxic, on-pathway intermediates. Based on these observations, we presented a model for the inhibition of tau, α-synuclein and Aβ aggregation by small molecules. Ehrnhoefer et al. recently presented a different model for the inhibition of fibril formation of α-synuclein and Aβ by the small molecule inhibitor (−)-epigallocatechin-3-gallate (EGCG) [11]. They reported that EGCG inhibited the assembly of α-synuclein and Aβ by binding to natively unfolded protein monomers, preventing their conversion into toxic on-pathway aggregation intermediates. Instead, α-synuclein and Aβ formed unstructured, non-toxic oligomers that were said to be off-pathway.

In this study, we used 10 epitope-specific antibodies of α-synuclein spanning the whole of α-synuclein and investigated their reactivities with monomeric α-synuclein and with α-synuclein fibrils. Some antibodies detected conformational changes that distinguished monomers from fibrils. These antibodies were then used to detect conformational changes in polyphenol-stabilized monomers and dimers of α-synuclein. Importantly, SDS-stable, polyphenol-stabilized monomers and dimers showed an intermediate reactivity between that of monomers and fibrils. These findings indicate that inhibitory compounds bind and stabilize on-pathway intermediates of amyloid fibril formation.

* Corresponding authors. Fax: +81 3 3329 8035.
E-mail addresses: masato@prit.go.jp (M. Hasegawa), mg@mrc-lmb.cam.ac.uk (M. Goedert).

0014-5793/$34.00
doi:10.1016/j.febslet.2009.01.037

2. Materials and methods

2.1. Antibodies

Polyclonal antibodies were raised against synthetic peptides corresponding to residues 1–10, 11–20, 21–30, 31–40, 41–50, 51–60, 61–70, 75–91 and 131–140 of human α-synuclein, with Cys at the C-terminus or the N-terminus (Greiner Bio-One Co. Ltd.) (Table 1). The peptides were conjugated to *m*-maleimidobenzoyl-*N*-hydrosuccinimide ester-activated keyhole limpet hemocyanin (KLH). The KLH-peptide complex (1 mg of each immunogen) emulsified in Freund's complete adjuvant was injected subcutaneously into a New Zealand White rabbit, followed by 5 weekly subcutaneous injections of 150 μg KLH-peptide complex emulsified in Freund's incomplete adjuvant, starting 3 weeks after the first immunization. Antibody Syn259, which recognizes residues 104–119 of α-synuclein, was kindly provided by Dr. S. Nakajo.

2.2. Expression and purification of α-synuclein

Human α-synuclein was expressed in *E. coli* BL21 (DE3) cells, as described [9]. To avoid the production of α-synuclein dimers induced by misexpression of cysteine-containing α-synuclein, the Y136-TAT construct was used [12]. α-Synuclein was purified by boiling, Q-Sepharose ion exchange chromatography and ammonium sulfate precipitation, followed by dialysis against 30 mM Tris–HCl, pH 7.5, and the determination of protein concentrations, as described [9].

2.3. Preparation of α-synuclein fibrils and inhibitor-bound monomers and dimers

Purified α-synuclein (7 mg/ml) was incubated at 37 °C in a shaking incubator (200 rpm) in 30 mM Tris–HCl, pH 7.5, containing 0.1% NaN_3 for 72 h. Fibrils were pelleted by spinning the assembly mixtures at 113000×*g* for 20 min. To prepare SDS-stable, inhibitor-bound monomers and dimers, the polyphenol exifone was used in most experiments [9]. Similar results were obtained with dopamine and gossypetin, two previously described inhibitory compounds [4,9]. Exifone-bound α-synuclein monomers (Exi-monomer) and dimers (Exi-dimer) were prepared by gel filtration, as described [9]. Briefly, α-synuclein (7 mg/ml) was incubated in the presence of 2 mM inhibitory compound at 37 °C for 72 h in 30 mM Tris-HCl containing 0.1% sodium azide, and centrifuged at 113000×*g* for 20 min. The supernatants were loaded onto a Superdex 200 gel filtration column (1 × 30 cm), eluted in 10 mM Tris–HCl, pH 7.5, containing 150 mM NaCl, and monitored at 214 nm. Fractionated samples were analyzed by SDS–PAGE and immunoblotting. Protein concentrations were determined as described [9].

Table 1
Antigen peptides for immunization of rabbits.

Name of antibodies	AA residues	Antigen peptide
Syn1-10	1–10	MDVFMKGLSKC
Syn11-20	11–20	AKEGVVAAAEC
Syn21-30	21–30	KTKQGVAEAAC
Syn31-40	31–40	GKTKEGVLYVC
Syn41-50	41–50	GSKTKEGVVHC
Syn51-60	51–60	GVATVAEKTKC
Syn61-70	61–70	EQVTNVGGAVC
Syn75-91	75–91	CTAVAQKTVEGAGSIAAA
Syn131-140	131–140	CEGYQDYEPEA

2.4. ELISA and dot blot assay

For the ELISA, peptide immunogens, α-synuclein monomers and fibrils, as well as Exi-monomers and dimers (0.5–1.0 μg/well in 50 mM Tris–HCl, pH 8.8) were coated onto microtitre plates (SUMILON) at 4 °C for 16 h. The plates were blocked with 10% fetal bovine serum (FBS) in PBS, incubated with the first antibody diluted in 10% FBS/PBS at room temperature for 1.5 h, followed by incubation with HRP-goat anti-rabbit IgG (Bio-Rad) at 1:1000 dilution, and reacted with the substrate, 0.4 mg/ml *o*-phenylendiamine, in citrate buffer (24 mM citric acid, 51 mM Na_2HPO_4). The absorbance at 490 nm was measured using Plate Chameleon (HIDEX). For the dot blot assay, 100 ng α-synuclein was spotted onto a PVDF membrane by using a dot blot apparatus (Bio-Rad). Membranes were stained with Coomassie Brilliant Blue or blocked with 3% gelatin/PBS and incubated overnight at room temperature with anti-α-synuclein antibodies in 10% FBS/PBS. Immunoreactivity was detected with avidin-biotin (Vector Laboratories) and developed using NiCl-enhanced diaminobenzidine. The rate of reactivity was quantified by scanning densitometry and expressed relative to the density of α-synuclein fibrils (taken as 100%).

3. Results

3.1. Antibody specificities

In order to detect conformational changes in α-synuclein, antibodies were raised against nine peptides (corresponding to residues 1–10, 11–20, 21–30, 31–40, 41–50, 51–60, 61–70, 75–91 and 131–140) (Table 1). The specificities of the antibodies were analyzed by ELISA. The peptides used as immunogens were coated on a plate and probed with each antibody. As shown in Fig. 1, each antibody reacted strongly with the appropriate peptide, but hardly with the other peptides. Antibody Syn41–50 was an exception, in that it weakly recognized peptides 11–20 and 31–40, in addition to recognizing peptide 41–50 very strongly.

3.2. Analysis of conformational changes in α-synuclein using epitope-specific antibodies

We investigated the reactivity of monomeric α-synuclein and of α-synuclein fibrils by dot blot assay using the nine antibodies described above and antibody Syn259 whose epitope corresponds to residues 104–119 of α-synuclein. Monomeric α-synuclein was strongly detected by antibodies to the C-terminal region (Syn259 and Syn131–140), but not by antibodies to the N-terminal or middle region (Fig. 2). This is in good agreement with previous reports showing that the C-terminal region of α-synuclein is unfolded and shields the N-terminal and central regions by way of long-range intramolecular interactions [13,14]. In contrast, α-synuclein fibrils were strongly immunoreactive with all antibodies (Fig. 2), indicating that the relevant epitopes were accessible. This is also consistent with current knowledge of the location of individual β-strands and their connecting loops in the structure of the α -synuclein fibril [15,16]. These results indicate that conformational changes undergone by α-synuclein as it assembles into fibrils can be detected immunochemically. We next analyzed the conformations of exifone-stabilized monomers and dimers of α-synuclein, following their separation by gel filtration chromatography (Supplementary Fig.). SDS-stable dimers formed in the presence of exifone were recognized by antibodies specific for Syn1–10, Syn11–20, Syn21–30, Syn31–40 and Syn41–50 (Fig. 2). They were less well recognized by antibodies specific for Syn51–60, Syn61–70 and Syn75–91. The antibody recognition patterns of SDS-stable monomers formed in the presence of exifone were intermediate between

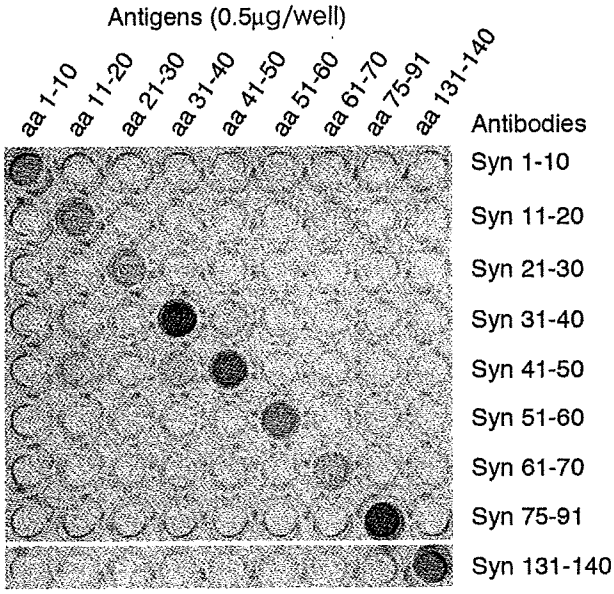

Fig. 1. Specificities of anti-peptide antibodies spanning the whole of α-synuclein determined by ELISA. Synthetic peptides (0.5 μg/well) were coated on a 96-well microtitre plate for 16 h at 4 °C and each of the 9 peptides was probed with each of the 9 antisera.

those of untreated monomers and polyphenol-stabilized dimers (Fig. 2). All antibodies gave similar results by ELISA (data not shown).

4. Discussion

We show here that the conformational changes undergone by α-synuclein during the conversion from monomers to amyloid fibrils can be detected by epitope-specific antibodies. Antibodies to the C-terminal region of α-synuclein recognized monomers and fibrils almost equally, whereas antibodies to the N-terminal region strongly reacted with fibrils, but labelled monomers only weakly. Under physiological conditions, α-synuclein is known to populate an ensemble of conformations, including conformers that are more compact than expected for a random coil protein [17–19]. Our findings indicating that the N-terminal region is buried and only poorly accessible to antibodies, are in line with this work. They are also in agreement with reports showing that the C-terminal region of α-synuclein is unfolded and shields the N-terminal and central regions by way of long-range intramolecular interactions [13,14].

The core of the fibril spans approximately residues 30–100 of α-synuclein [20,21] and is believed to comprise five parallel β-strands that are separated by flexible loops [16]. Our findings on α-synuclein fibrils are consistent with the loop regions being antibody-accessible. Conformational changes detectable by specific antibodies have previously been reported in tau, another natively unfolded protein, as it assembles into abnormal filaments. Thus, antibody Alz50 reacts more strongly with paired helical filament tau from Alzheimer's disease brain than with the soluble monomeric protein [22].

Inhibitor-bound dimers and monomers of α-synuclein were tested using the same panel of antibodies. When bound to the polyphenol exifone, dimers of α-synuclein were detected by antibodies to the N-terminal region in a manner similar to fibrils. Unlike the latter, inhibitor-bound dimers were not recognized by antibodies to the middle region of α-synuclein. Antibodies to the C-terminal region recognized inhibitor-bound dimers and fibrils equally. Relative to unbound monomers, therefore, inhibitor-bound α-synuclein dimers are characterized by a more accessible N-terminal region. NMR spectroscopy of exifone-stabilized α-synuclein dimers and nitroblue tetrazolium staining of cleaved exifone-bound α-

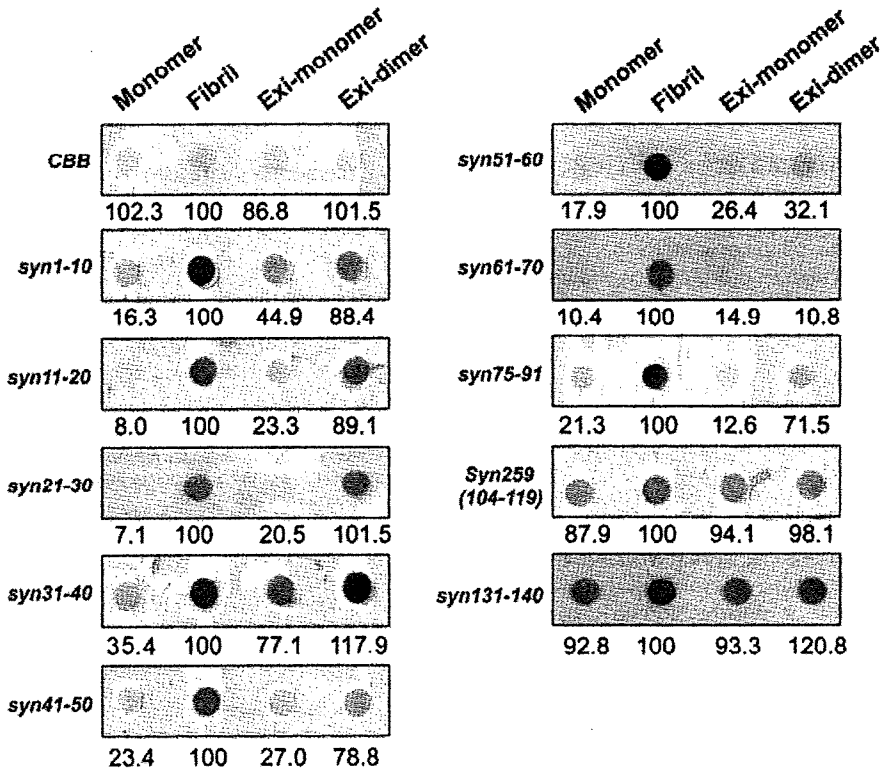

Fig. 2. Dot blot analysis of monomeric α-synuclein, the α-synuclein fibril, as well as exifone-stabilized α-synuclein monomers (Exi-monomer) and dimers (Exi-dimer), with 10 antibodies whose epitopes span the whole of human α-synuclein. The relative intensities of immunoreactivity are indicated below the dots and expressed as % of fibril immunoreactivity (taken as 100, $n = 3$). Each dot corresponds o 100 ng of α-synuclein.

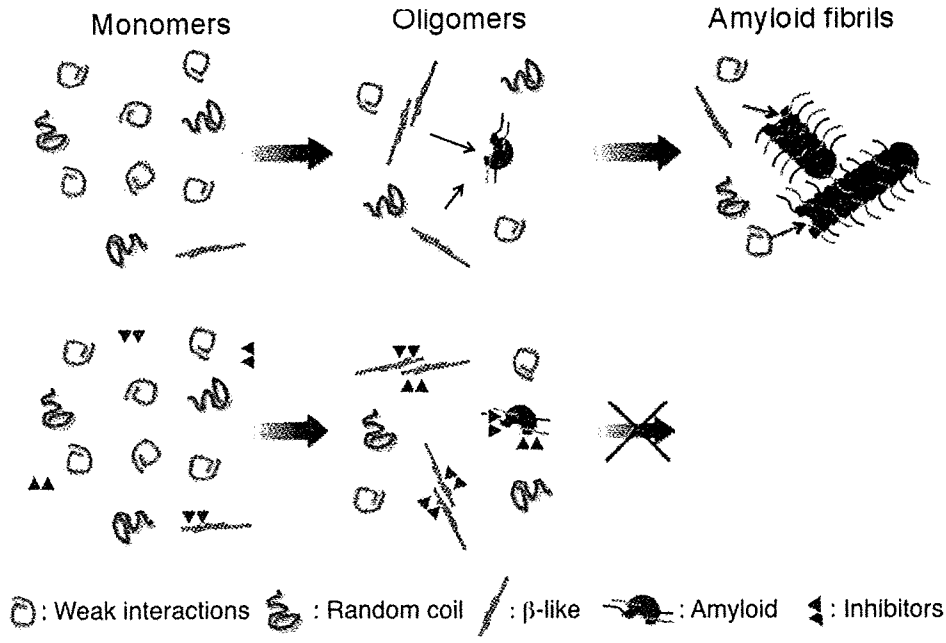

Fig. 3. Model of the inhibition of α-synuclein fibril formation by small molecules.

synuclein showed that N-terminal regions are involved in dimer formation and that exifone binds to these regions (in preparation). Dimers of α-synuclein are believed to play a key role in the aggregation process [23]. A recent study has also shown that aggregation-inhibiting molecules interact with N-terminal regions of α-synuclein [24]. When tested with the panel of antibodies, inhibitor-bound monomers of α-synuclein gave a pattern intermediate between that of unbound monomers and inhibitor-bound dimers. Taken together, our findings suggest the existence of a linear pathway leading from monomeric to fibrillar α-synuclein, with exifone binding to misfolded monomers and dimers, thereby preventing fibril formation. A similar mechanism may underlie the inhibition of α-synuclein fibril formation by the molecular chaperone Hsp70 [25].

This interpretation is at odds with a recent study reporting that oligomers of α-synuclein and Aβ formed in the presence of EGCG were off-pathway [11]. In this study, conformation-specific antibody A11, which recognizes an oligomeric state that is believed to be common to many amyloidogenic proteins [26], did not detect EGCG-induced oligomers. This antibody is believed to be specific for on-pathway toxic oligomers of α-synuclein. However, Ehrnhoefer et al. found that it recognized His-tagged monomeric α-synuclein [11]. In our hands, antibody A11 also recognized α-synuclein fibrils (unpublished observation).

Single molecule studies have shown that α-synuclein exists as three distinct conformers *in vitro* that are characterized by: long-distance weak interactions, random coil and β-like structures [27]. The β-like conformer has been linked to the process of α-synuclein aggregation. It is tempting to suggest that exifone binds to this conformer, in line with the finding that inhibitory compounds inhibit amyloid fibril formation at substoichiometric concentrations [8,9]. Our previous work on the ordered aggregation of tau protein has also shown that small molecule inhibitors bind to oligomers and filaments, but not to native monomers [8]. A revised model for the inhibition of α-synuclein fibril formation by small molecules is shown in Fig. 3. Monomeric α-synuclein exists in a native conformation, with a small proportion of β-like structure. During assembly, the latter may dimerize, oligomerize and form amyloid seeds. Amyloid fibrils can grow from these seeds. Small molecule inhibitors bind to misfolded monomers, dimers and oligomers, thus preventing fibril formation.

Acknowledgements

This work was supported by a Grant-in-aid for Scientific Research on Priority Areas – Research on Pathomechanisms of Brain Disorders (to M.H., 20023038) and Grants-in-aid for Scientific Research (B) (to M.H., 18300117) and (C) (to T.N.) from the Ministry of Education, Culture, Sports, Science and Technology of Japan.

Appendix A. Supplementary data

Supplementary data associated with this article can be found, in the online version, at doi:10.1016/j.febslet.2009.01.037.

References

[1] Goedert, M. and Spillantini, M.G. (2006) A century of Alzheimer's disease. Science 314, 777–781.
[2] Goedert, M. (2001) α-Synuclein and neurodegenerative diseases. Nature Rev. Neurosci. 2, 492–501.
[3] Findeis, M.A. (2000) Approaches to discovery and characterization of inhibitors of amyloid β-peptide polymerization. Biochim. Biophys. Acta 1502, 76–84.
[4] Conway, K.A., Rochet, J.C., Bieganski, R.M. and Lansbury, P.T. (2001) Kinetic stabilization of the α-synuclein protofibril by a dopamine-α-synuclein adduct. Science 294, 1346–1349.
[5] Heiser, V., Engemann, S., Bröcker, W., Dunkel, I., Boeddrich, A., Waelter, S., Nordhoff, E., Lurz, R., Schugardt, N., Rautenberg, S., Herhaus, C., Barnickel, G., Böttcher, H., Lehrach, H. and Wanker, E.E. (2002) Identification of benzothiazoles as potential polyglutamine aggregation inhibitors of Huntington's disease by using an automated filter retardation assay. Proc. Natl. Acad. Sci. USA 99, 16400–16406.
[6] Cashman, N.R. and Caughey, B. (2004) Prion diseases: close to effective therapy? Nat. Rev. Drug Discov. 3, 874–884.
[7] Pickhardt, M., Gazova, Z., von Bergen, M., Khlistunova, I., Wang, Y., Hascher, A., Mandelkow, E.M., Biernat, J. and Mandelkow, E. (2005) Anthraquinones inhibit tau aggregation and dissolve Alzheimer's paired helical filaments *in vitro* and in cells. J. Biol. Chem. 280, 3628–3635.
[8] Taniguchi, S., Suzuki, N., Masuda, M., Hisanaga, S., Iwatsubo, T., Goedert, M. and Hasegawa, M. (2005) Inhibition of heparin-induced tau filament formation by phenothiazines, polyphenols, and porphyrins. J. Biol. Chem. 280, 7614–7623.

[9] Masuda, M., Suzuki, N., Taniguchi, S., Oikawa, T., Nonaka, T., Iwatsubo, T., Hisanaga, S.-I., Goedert, M. and Hasegawa, M. (2006) Small molecule inhibitors of α-synuclein filament assembly. Biochemistry 45, 6085–6094.
[10] Hong, D.-P., Fink, A.L. and Uversky, V.N. (2008) Structural characteristics of α-synuclein oligomers stabilized by the flavonoid baicalein. J. Mol. Biol. 383, 214–223.
[11] Ehrnhoefer, D.E., Bieschke, J., Boeddrich, A., Herbst, M., Masino, L., Lurz, R., Engemann, S., Pastore, A. and Wanker, E.E. (2008) EGCG redirects amyloidogenic polypeptides into unstructured, off-pathway oligomers. Nat. Struct. Mol. Biol. 15, 558–566.
[12] Masuda, M., Dohmae, N., Nonaka, T., Oikawa, T., Hisanaga, S.-I., Goedert, M. and Hasegawa, M. (2006) Cysteine misincorporation in bacterially expressed human α-synuclein. FEBS Lett. 580, 1775–1779.
[13] Dedmon, M.M., Lindorff-Larsen, K., Christodoulou, J., Vendruscolo, M. and Dobson, C.M. (2005) Mapping long-range interactions in α-synuclein using spin-label NMR and ensemble molecular dynamics simulations. J. Am. Chem. Soc. 127, 476–477.
[14] Bertoncini, C.W., Jung, Y.S., Fernandez, C.O., Hoyer, W., Griesinger, C., Jovin, T.M. and Zweckstetter, M. (2005) Release of long-range tertiary interactions potentiates aggregation of natively unstructured α-synuclein. Proc. Natl. Acad. Sci. USA 102, 1430–1435.
[15] Heise, H., Hoyer, W., Becker, S., Andronesi, O.C., Riedel, D. and Baldus, M. (2005) Molecular-level secondary structure, polymorphism, and dynamics of full-length α-synuclein fibrils studied by solid-state NMR. Proc. Natl. Acad. Sci. USA 102, 15871–15876.
[16] Vilar, M., Chou, H.-T., Lührs, T., Maji, S.K., Riek-Loher, D., Verel, R., Manning, G., Stahlberg, H. and Riek, R. (2008) The fold of α-synuclein fibrils. Proc. Natl. Acad. Sci. USA 105, 8637–8642.
[17] Syme, C.D., Blanch, E.W., Holt, C., Jakes, R., Goedert, M., Hecht, L. and Barron, L.D. (2001) A Raman optical activity study of rheomorphism in caseins, synucleins and tau: New insight into the structure and behaviour of natively unfolded proteins. Eur. J. Biochem. 269, 148–156.
[18] Maiti, N.C., Apetrui, M.M., Zagorski, M.G., Carey, P.R. and Anderson, V.R. (2004) Raman spectroscopic characterization of secondary structure in natively unfolded proteins: α-Synuclein. J. Am. Chem. Soc. 126, 2399–2408.
[19] Lee, J.C., Langen, R., Hummal, P.A., Gray, H.B. and Winkler, J.R. (2004) α-Synuclein structures from fluorescence energy-transfer kinetics: Implications for the role of the protein in Parkinson's disease. Proc. Natl. Acad. Sci. USA 101, 16466–16471.
[20] Miake, H., Mizusawa, H., Iwatsubo, T. and Hasegawa, M. (2002) Biochemical characterization of the core structure of α-synuclein filaments. J. Biol. Chem. 277, 19213–19219.
[21] Der-Sarkissian, A., Jao, C.C., Chen, J. and Langen, R. (2003) Structural organization of α-synuclein fibril structure studied by site-directed spin labeling. J. Biol. Chem. 278, 24970–24979.
[22] Carmel, G., Mager, E.M., Binder, L.I. and Kuret, J. (1996) The structural basis of monoclonal antibody Alz50's selectivity for Alzheimer's disease pathology. J. Biol. Chem. 271, 32789–32795.
[23] Yu, J., Malkova, S. and Lyubchenko, Y.L. (2008) α-Synuclein misfolding: single molecule AFM force spectroscopy study. J. Mol. Biol. 384, 992–1001.
[24] Rao, J.N., Dua, V. and Ulmer, T.S. (2008) Characterization of α-synuclein interactions with selected aggregation-inhibiting small molecules. Biochemistry 47, 4651–4656.
[25] Luk, K.C., Mills, I.P., Trojanowski, J.Q. and Lee, V.M.-Y. (2008) Interactions between Hsp70 and the hydrophobic core of α-synuclein inhibit fibril assembly. Biochemistry 47, 12614–12625.
[26] Kayed, R., Head, E., Thompson, J.L., McIntire, T.M., Milton, S.C., Cotman, C.W. and Glabe, C.G. (2003) Common structure of soluble amyloid oligomers implies common mechanism of pathogenesis. Science 300, 486–489.
[27] Sandal, M., Valle, F., Tessari, I., Mammi, S., Bergantino, E., Musiani, F., Brucale, M., Bubacco, L. and Samori, B. (2008) Conformational equilibria in monomeric α-synuclein at the single-molecule level. PLoS Biol. 6, e6.

FEBS Letters 583 (2009) 2419–2424

ELSEVIER

FEBS Letters

journal homepage: www.FEBSLetters.org

Methylene blue and dimebon inhibit aggregation of TDP-43 in cellular models

Makiko Yamashita [a,1], Takashi Nonaka [a,1], Tetsuaki Arai [b], Fuyuki Kametani [a], Vladimir L. Buchman [c], Natalia Ninkina [c,d], Sergey O. Bachurin [d], Haruhiko Akiyama [b], Michel Goedert [e], Masato Hasegawa [a,*]

[a] Department of Molecular Neurobiology, Tokyo Institute of Psychiatry, Tokyo Metropolitan Organization for Medical Reearch, 2-1-8 Kamikitazawa, Setagaya-ku, Tokyo 156-8585, Japan
[b] Department of Psychogeriatrics, Tokyo Institute of Psychiatry, Tokyo Metropolitan Organization for Medical Research, 2-1-8 Kamikitazawa, Setagaya-ku, Tokyo 156-8585, Japan
[c] School of Biosciences, Cardiff University, Cardiff CF10 3US, UK
[d] Institute of Physiologically Active Compounds, RAS, Chernogolovka 142432, Russian Federation
[e] MRC Laboratory of Molecular Biology, Hills Road, Cambridge CB2 0QH, UK

ARTICLE INFO

Article history:
Received 18 May 2009
Revised 10 June 2009
Accepted 22 June 2009
Available online 26 June 2009

Edited by Jesus Avila

Keywords:
Tau
Alpha-synuclein
Inhibitor
Alzheimer
ALS
FTLD

ABSTRACT

Amyotrophic lateral sclerosis (ALS) and frontotemporal lobar degeneration with ubiquitinated inclusions (FTLD-U) are major neurodegenerative diseases with TDP-43 pathology. Here we investigated the effects of methylene blue (MB) and dimebon, two compounds that have been reported to be beneficial in phase II clinical trials of Alzheimer's disease (AD), on the formation of TDP-43 aggregates in SH-SY5Y cells. Following treatment with 0.05 μM MB or 5 μM dimebon, the number of TDP-43 aggregates was reduced by 50% and 45%, respectively. The combined use of MB and dimebon resulted in a 80% reduction in the number. These findings were confirmed by immunoblot analysis. The results indicate that MB and dimebon may be useful for the treatment of ALS, FTLD-U and other TDP-43 proteinopathies.

1. Introduction

Amyotrophic lateral sclerosis (ALS) is a neurodegenerative disease that is characterized by progressive weakness and muscle wasting, and for which no effective therapies exist. Frontotemporal lobar degeneration (FTLD) is the second most common form of dementia after Alzheimer's disease (AD) in the population below the age of 65 years. In many cases with these disorders, ubiquitin (Ub)-positive, tau-negative intracytoplasmic inclusions form in nerve cells and glial cells. TAR DNA binding protein of 43 kDa (TDP-43) is the major component of these inclusions [1–3]. Biochemical and histological analyses demonstrated that TDP-43 accumulates in brain and spinal cord in a hyperphosphorylated and fibrillar form [4]. Furthermore, missense mutations in the TDP-43 gene have been identified in familial cases of ALS and ALS with FTLD-U [5–9]. Together, these findings indicate that dysfunction of TDP-43 is central to the etiology and pathogenesis of ALS and FTLD-U. In addition, TDP-43 has also been found to accumulate in other neurodegenerative disorders, including AD, dementia with Lewy bodies [10], Parkinsonism-dementia complex of Guam [11], argyrophilic grain disease [12], Huntington's disease [13], Perry syndrome [14] and familial British dementia [15].

Inhibition of the aggregation of TDP-43 and promotion of its clearance are considered to be major therapeutic avenues for ALS and FTLD-U. As for other neurodegenerative diseases, current tools include antibodies, synthetic peptides, molecular chaperones and chemical compounds. Of the latter, methylene blue (MB) and dimebon have recently been reported to have significant beneficial effects in phase II clinical trials of AD [16,17]. MB is a phenothiazine compound that has been used for treating methemoglobinemia [18,19], inhibiting nitric oxide synthase [20], reducing nGMP [21], enhancing β-oxydation in mitochondria [22], inhibiting of noradrenaline re-uptake [23] and enhancing brain mitochondrial cytochrome oxidase activity [24,25]. It has also been shown to inhibit AD-like Aβ and tau aggregation in vitro [26,27]. Dimebon is a non-selective anti-histaminergic compound that was in clinical use for many years before more selective agents became available [28]. It has been reported to inhibit butyrylcholinesterase, acetylcholinesterase, NMDA receptors, voltage-gated calcium channels, adrenergic receptors, histamine H1 receptors, histamine H2 receptors and serotonin receptors, as well as to stabilize glutamate-induced Ca^{2+} signals [29–31]. The effects of dimebon on pathological protein aggregation have not been studied in detail, but recently we demonstrated that chronic administration of this drug reduced

* Corresponding author. Fax: +81 3 3329 8035.
E-mail address: masato@prit.go.jp (M. Hasegawa).
[1] These authors contributed equally to this work.

0014-5793/$36.00
doi:10.1016/j.febslet.2009.06.042

the number of nerve cell deposits in a mouse model of synucleinopathy [32].

Here we investigated whether MB and dimebon can reduce the formation of TDP-43 inclusions in SH-SY5Y cellular models. Significantly, the treatment of cells with each compound and their combined application inhibited the formation of TDP-43 aggregates, suggesting that MB and dimebon may be effective for the treatment of ALS and FTLD-U.

2. Materials and methods

2.1. Antibodies

A polyclonal anti-TDP-43 antibody (anti-TDP-43) was purchased from ProteinTech Group Inc. (10782-1-AP, Chicago, USA). A polyclonal antibody specific for phosphorylated TDP-43 (anti-pS409/410) (available from Cosmo Bio Co., Tokyo, Japan) [4] and an anti-Ub antibody (MAB1510, Chemicon, Billerica, USA) were used for the evaluation of pathological forms of TDP-43.

2.2. TDP-43 cellular models and addition of compounds

To investigate the effects of MB and dimebon on the formation of TDP-43 aggregates, we used two cellular models of TDP-43 proteinopathy. The first consists of SH-SY5Y cells expressing mutant TDP-43 that lacks both the nuclear localization signal (NLS) and residues 187–192 (ΔNLS&187-192). In these cells, round structures positive for both anti-pS409/410 and anti-Ub are observed [33]. The second model consists of SH-SY5Y cells expressing an aggregation-prone TDP-43 C-terminal fragment (residues 162–

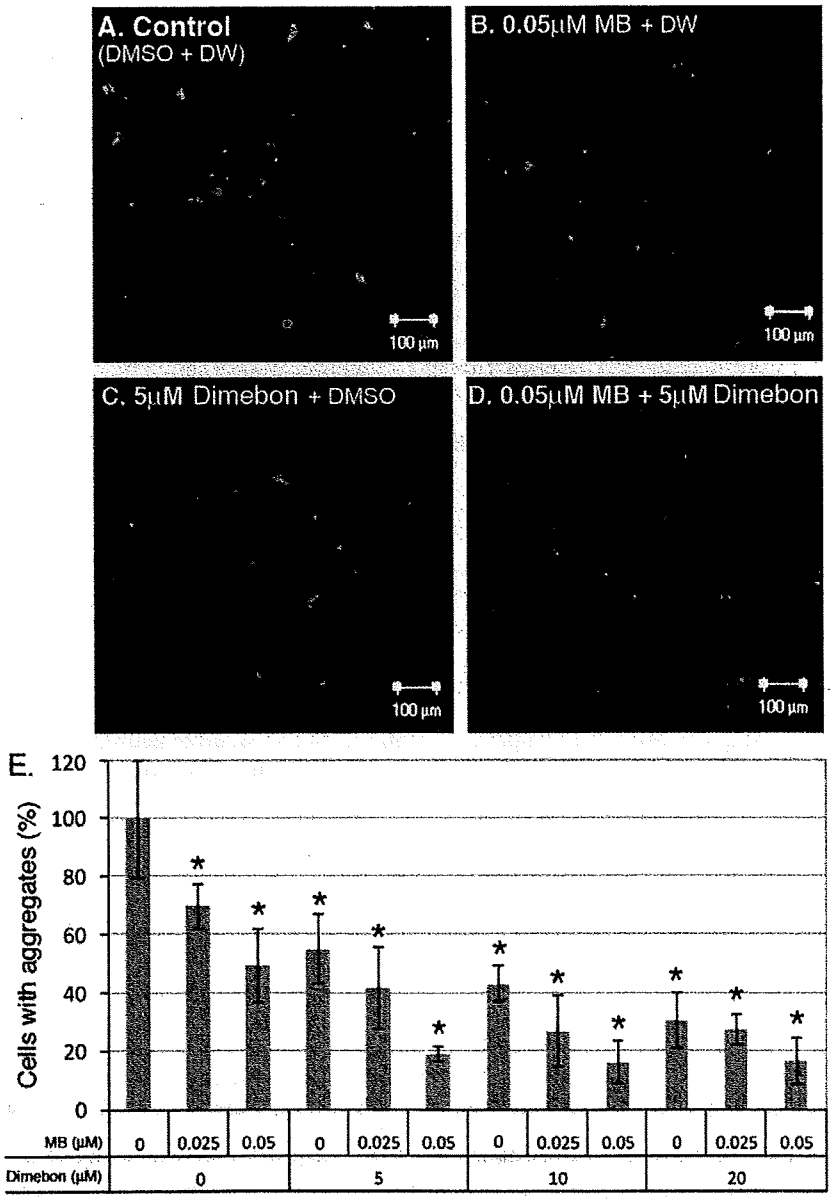

Fig. 1. Immunohistochemical analysis of the effects of methylene blue (MB) and dimebon on the aggregation of TDP-43 in SH-SY5Y cells expressing TDP-43 (ΔNLS&187-192). TDP-43 inclusions were stained with anti-pS409/410 antibody and detected with Alexa Fluor 488-labeled secondary antibody. Representative confocal images from cells treated with control (DMSO + DW) (A), 0.05 μM MB + DW (B), 5 μM dimebon + DMSO (C) and 0.05 μM MB + 5 μM dimebon (D) are shown. (E) Quantitation of cells with TDP-43 aggregates. The number of cells with intracellular TDP-43 aggregates was counted and expressed as the percentage of cells with aggregates in the absence of compound (taken as 100%). Fluorescence intensity within an area of approximately 800 μm × 800 μm was assessed by confocal microscopy. The intensity of Alexa Fluor 488 was calculated as the ratio of that of TO-PRO-3. At least 8 areas per sample were measured (n = 8–16). Data are means ± S.E.M. $^*P < 0.01$ by Student's t test.

414) as a green fluorescent protein (GFP)-fusion [34,35]. Its expression also results in the formation of anti-pS409/410- and anti-Ub-positive inclusions. Six hours after transfection, the cells were treated with MB (Sigma–Aldrich, St. Louis, USA) dissolved in dimethyl sulfoxide (DMSO), dimebon dissolved in sterile distilled water (DW) or MB + dimebon and cultured for 3 days. As controls, cells were treated with either DMSO or DW, or both of them for 3 days.

2.3. Immunohistochemical analysis

SH-SY5Y cells were grown on coverslips and transfected as described [33]. After incubation for the indicated times, the cells were fixed with 4% paraformaldehyde and stained with anti-phosphorylated TDP-43 antibody pS409/410 or anti-Ub, followed by Alexa Fluor 488- or Alexa Fluor 568-labeled IgG (Invitrogen, Carlsbad, USA). After washing, the cells were further incubated with TO-PRO-3 (Invitrogen, Carlsbad, USA) to stain nuclear DNA. To quantify the cells with TDP-43 aggregates, the laser power (at 488 nm for detection of Alexa Fluor 488 and GFP) was adjusted, so that only aggregates were detected as described [34]. Total intensity of fluorescence detected at the threshold laser power and that of TO-PRO-3 fluorescence, the latter corresponding to the total number of cells in a given field (approximately 800 μm × 800 μm), were measured with LSM5 Pascal v 4.0 software (Carl Zeiss), and the ratio of cells with inclusions calculated.

2.4. Immunoblot analysis

Tris saline (TS)-soluble, Triton X-100 (TX)-soluble and Sarkosyl (Sar)-soluble fractions, as well as the final pellet, were prepared,

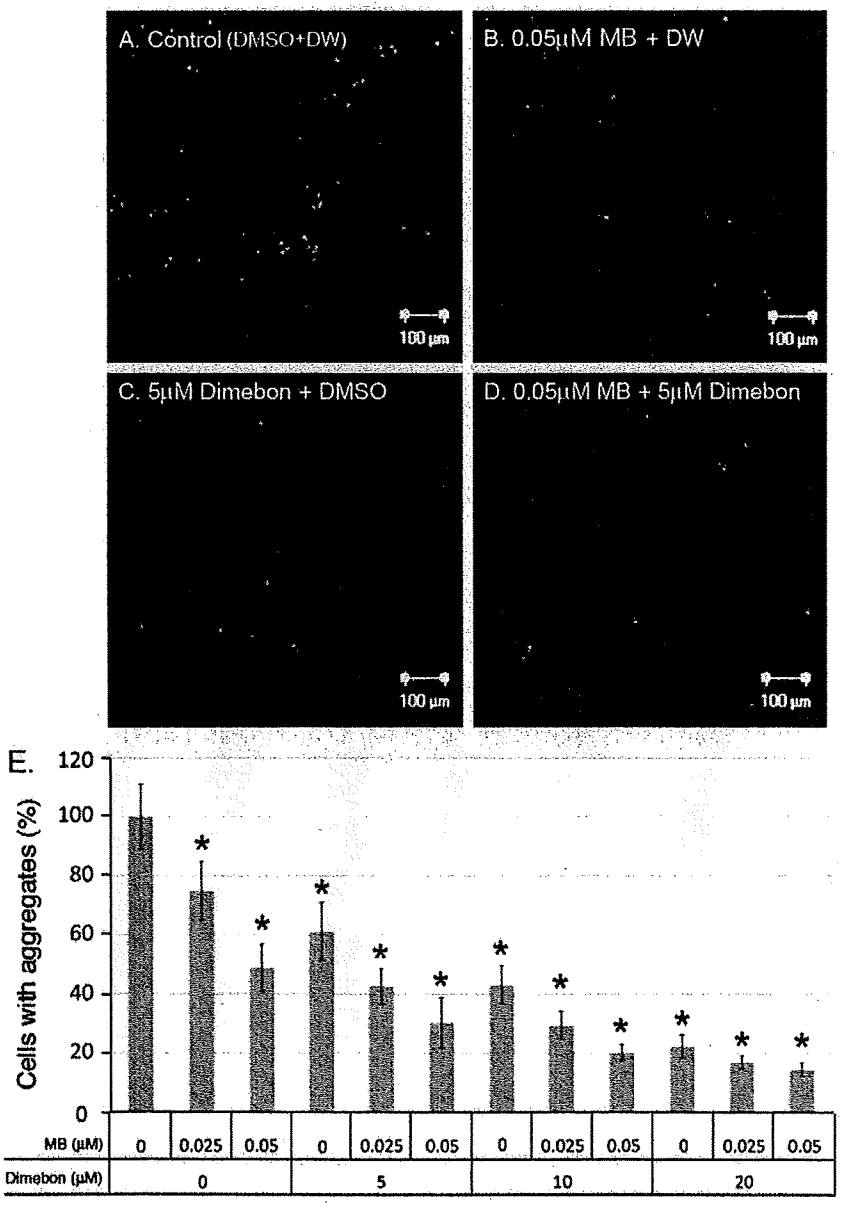

Fig. 2. Immunohistochemical analysis of the effects of methylene blue (MB) and dimebon on the aggregation of TDP-43 in SH-SY5Y cells expressing TDP-43 C-terminal fragment (162–414) as GFP fusion protein. TDP-43 inclusions were detected by fluorescence of GFP, when the laser power was adjusted. Representative confocal images from cells treated with control (DMSO + DW) (A), 0.05 μM MB + DW (B), 5 μM dimebon + DMSO (C) and 0.05 μM MB + 5 μM dimebon (D) are shown. (E) Quantitation of cells with TDP-43 aggregates. The intensity of fluorescence of GFP was calculated as the ratio of that of TOPRO-3. At least 8 areas per sample were measured ($n = 8–16$). Data are means ± S.E.M. $^*P < 0.01$ by Student's t test.

run on SDS–PAGE and immunoblotted with anti-TDP-43 and anti-pS409/410 antibodies, as described [33].

3. Results

3.1. Effects of MB and dimebon on the formation of TDP-43 inclusions

We first investigated the cytotoxicity of MB and dimebon. SH-SY5Y cells were treated with different concentrations of each compound, cultured for 1 day, followed by growth measurements. No toxic effects were detected with dimebon at concentrations of 1–60 μM, whereas a significant decrease in the number of cells was observed with MB at concentrations greater than 0.1 μM. Cells transfected with TDP-43 (ΔNLS&187-192) formed round intracellular inclusion-like structures that were positive with both anti-pS409/410 and anti-Ub antibodies, as reported previously [33] (Fig. 1A). When the cells were treated for 3 days with MB, dimebon or MB + dimebon, the number of TDP-43 inclusions was reduced (Fig. 1B–D). Compared to controls, we observed a 50% reduction in the number of inclusions with 0.05 μM MB, a 45% reduction with 5 μM dimebon and a 80% reduction with 0.05 μM MB + 5 μM dimebon (Fig. 1B–E). The effects were concentration-dependent and statistically significant (Fig. 1E). Thus, 10 μM dimebon caused a 60% reduction and 20 μM dimebon a 70% reduction in the number of TDP-43 inclusions. Similar results were obtained using a second cellular model of TDP-43 proteinopathy (Fig. 2), which expresses a C-terminal fragment (162–414) of TDP-43 as GFP fusion protein [34]. Other anti-histaminergic compounds, including promethazine hydrochloride, diphenhydramine hydrochloride (H1 histamine receptor antagonist) and thioperamide maleate (H3 histamine receptor antagonist) (Sigma–Aldrich, St. Louis, USA), did not affect the number of TDP-43 aggregates (Fig. 3). Similarly, two phenothiazine compounds tested, chlorpromazine hydrochloride and perphenazine (Sigma–Aldrich, St. Louis, USA), which failed to exert any effect on tau aggregation, did not affect the aggregation of TDP-43 (Fig. 3)

3.2. Immunoblot analysis of TDP-43 in cells treated with MB and dimebon

The immunohistochemical results were confirmed by immunoblotting. Cells expressing TDP-43 (ΔNLS&187-192) (data not shown) or the C-terminal fragment (162–414) of TDP-43 (Fig. 4) were sequentially extracted with TS, TX, and Sar, and the supernatants and pellets analyzed by immunoblotting. In cells transfected with the C-terminal fragment (162–414) of TDP-43, phosphorylated C-terminal fragment of TDP-43 was detected in the Sar-insoluble fraction, as reported previously [34] (black arrowhead in Fig 4A). The levels of this band with slower gel mobility were reduced when the cells were treated with MB, dimebon or MB + dimebon (Fig. 4A and B). By contrast, similar levels of endogenous TDP-43 (black arrow in Fig. 4A) and expressed C-terminal fragment of TDP-43 (white arrowhead in Fig. 4A) were detected in TS- and TX-soluble fractions of control cells and of cells treated with MB or dimebon, indicating that these compounds did not affect the amount of TDP-43.

4. Discussion

In this study, we examined the effects of two compounds, MB and dimebon, on the formation of abnormally phosphorylated TDP-43 inclusions using SH-SY5Y cellular models. Both compounds, when used singly or in combination, significantly reduced the number of TDP-43 aggregates. Although its mechanism of action remains to be clarified, it is reasonable to speculate that MB may bind to dimers and oligomers of TDP-43 and thereby inhibit fibril formation, as has previously been demonstrated for the inhibition of Aβ and tau aggregation by MB in vitro [27]. The present findings show, for the first time, that MB can reduce protein aggregation in cells.

In addition, we have identified dimebon as a compound capable of inhibiting the formation of abnormal inclusions of TDP-43. In view of the recent demonstration of its efficacy in a phase II

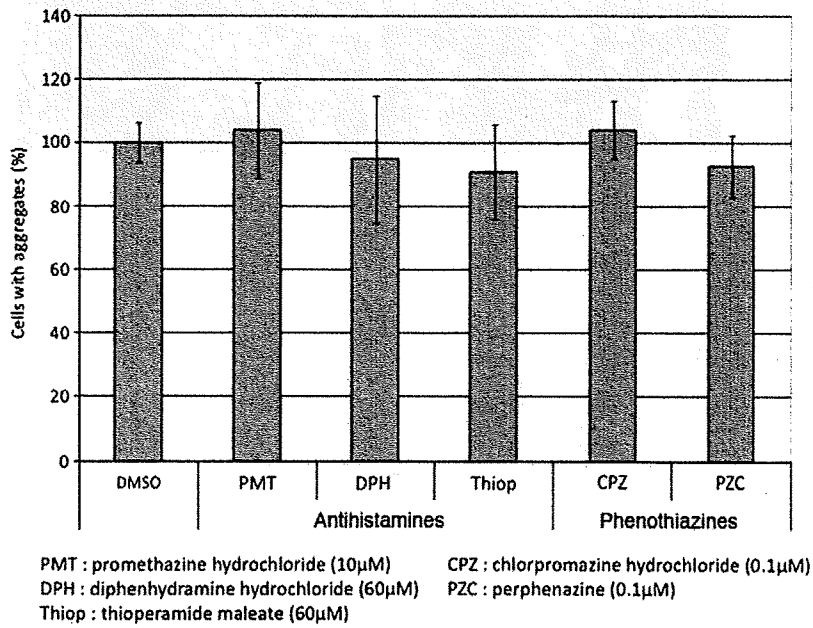

Fig. 3. Immunohistochemical analysis of the effects of three anti-histaminergic compounds, promethazine hydrochloride (PMT), diphenhydramine hydrochloride (DPH) and thioperamide maleate (Thiop), and two phenothiazine compounds, chlorpromazine hydrochloride (CPZ) and perphenazine (PZC) on the aggregation of TDP-43 in SH-SY5Y cells expressing GFP-fused TDP-43 C-terminal fragment (162–414) as GFP fusion protein. Quantitation of cells with TDP-43 aggregates is shown. No reduction in the TDP-43 aggregation was observed with these compounds. Promethazine hydrochloride and phenothiazines were tested at 10 μM and 0.1 μM, respectively, because they were toxic at higher concentrations.

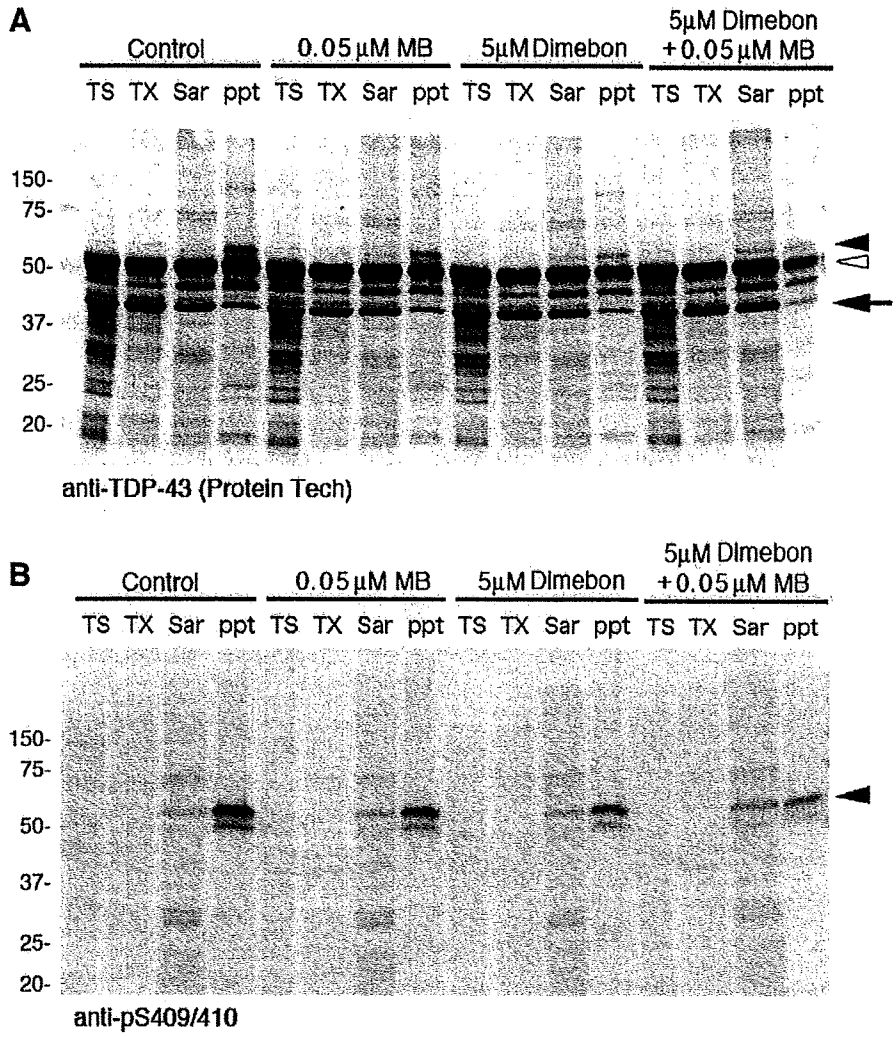

ig. 4. Immunoblot analysis of the effects of methylene blue (MB) and dimebon on the aggregation of TDP-43 in SH-SY5Y cells expressing GFP-tagged TDP-43 C-terminal ragment (162–414). Tris saline (TS)-soluble material, Triton X-100 (TX)-soluble material, Sarkosyl (Sar)-soluble material and the remaining pellet (ppt) were prepared from ontrol cells and from cells treated with 0.05 μM MB, 5 μM dimebon or 0.05 μM MB + 5 μM dimebon, run on SDS–PAGE and immunoblotted with anti-TDP-43 antibody (A) or nti-pS409/410 antibody (B). Abnormally phosphorylated TDP-43 C-terminal fragment (162–414) with a higher apparent molecular mass than the corresponding non-hosphorylated fragment (white arrowhead) was detected by both antibodies (black arrowheads). Similar levels of the non-phosphorylated GFP-tagged C-terminal fragment f TDP-43 (white arrowhead) and of endogenous TDP-43 (black arrow) were detected with the anti-TDP-43 antibody (A).

linical trial, dimebon may well become a new drug for the treatnent of AD and other neurodegenerative diseases. Although there ıave been some reports suggesting that dimebon may act as a ıeuroprotective agent and prevent mitochondrial pore transition n experimental models of AD [36] and Huntington's disease 30], its precise mode of action remains unknown. The present tudy suggests that dimebon may act by reducing the production ır accumulation of abnormal protein aggregates. It remains to be letermined whether the effects on TDP-43 aggregation are of a lirect or an indirect nature. It will also be interesting to investiate the effects of dimebon in existing [37] and future animal nodels of TDP-43 proteinopathy. We could not detect a signifiant effect of dimebon on the in vitro assembly of recombinant ıuman α-synuclein into filaments and on the heparin-induced ıssembly of recombinant human tau into filaments (data not hown). The recent demonstration that dimebon reduces the ıumber of protein inclusions in a model synucleinopathy [32] uggests that its effects may be indirect.

MB has been used for many years to treat a variety of condiions, including methemoglobinemia [19], septic shock [20] and lepression [38]. It has recently been used in a phase II trial of AD [16]. Furthermore, MB has been reported to have activity as an enhancer of mitochondrial activity [24], and a recent study has reported that it delays cellular senescence in cultured human fibroblasts [25]. However, high doses of MB are known to be toxic and to cause the formation of Heinz bodies in erythrocytes in infants [39]. A combination therapy, like the one used here, may therefore be advantageous.

In conclusion, the present results showing a reduction in the number of TDP-43 inclusions following the addition of MB and/or dimebon to transfected SH-SY5Y cells suggest that these compounds may be beneficial for the treatment of ALS and FTLD-U.

Acknowledgements

We thank Dr. Shahin Zibaee for helpful comments on the manuscript. This work was supported by a Grant-in-aid for Scientific Research on Priority Area – Research on Pathomechanisms of Brain Disorders (to M.H., 20023038) from Ministry of Education, Culture, Sports, Science and Technology and grants from Ministry of Health, Labor and Welfare of Japan, and a Russian Foundation for Basic Research Grant (to N.N., 09-04-01412-a).

References

[1] Neumann, M., Sampathu, D.M., Kwong, L.K., Truax, A.C., Micsenyi, M.C., Chou, T.T., Bruce, J., Schuck, T., Grossman, M., Clark, C.M., McCluskey, L.F., Miller, B.L., Masliah, E., Mackenzie, I.R., Feldman, H., Feiden, W., Kretzschmar, H.A., Trojanowski, J.Q. and Lee, V.M. (2006) Ubiquitinated TDP-43 in frontotemporal lobar degeneration and amyotrophic lateral sclerosis. Science 314, 130–133.

[2] Arai, T., Hasegawa, M., Akiyama, H., Ikeda, K., Nonaka, T., Mori, H., Mann, D., Tsuchiya, K., Yoshida, M., Hashizume, Y. and Oda, T. (2006) TDP-43 is a component of ubiquitin-positive tau-negative inclusions in frontotemporal lobar degeneration and amyotrophic lateral sclerosis. Biochem. Biophys. Res. Commun. 351, 602–611.

[3] Davidson, Y., Kelley, T., Mackenzie, I.R., Pickering-Brown, S., Du Plessis, D., Neary, D., Snowden, J.S. and Mann, D.M. (2007) Ubiquitinated pathological lesions in frontotemporal lobar degeneration contain the TAR DNA-binding protein. TDP-43. Acta Neuropathol. 113, 521–533.

[4] Hasegawa, M., Arai, T., Nonaka, T., Kametani, F., Yoshida, M., Hashizume, Y., Beach, T.G., Buratti, E., Baralle, F., Morita, M., Nakano, I., Oda, T., Tsuchiya, K. and Akiyama, H. (2008) Phosphorylated TDP-43 in frontotemporal lobar degeneration and amyotrophic lateral sclerosis. Ann. Neurol. 64, 60–70.

[5] Yokoseki, A., Shiga, A., Tan, C.F., Tagawa, A., Kaneko, H., Koyama, A., Eguchi, H., Tsujino, A., Ikeuchi, T., Kakita, A., Okamoto, K., Nishizawa, M., Takahashi, H. and Onodera, O. (2008) TDP-43 mutation in familial amyotrophic lateral sclerosis. Ann. Neurol. 63, 538–542.

[6] Sreedharan, J., Blair, I.P., Tripathi, V.B., Hu, X., Vance, C., Rogelj, B., Ackerley, S., Durnall, J.C., Williams, K.L., Buratti, E., Baralle, F., de Belleroche, J., Mitchell, J.D., Leigh, P.N., Al-Chalabi, A., Miller, C.C., Nicholson, G. and Shaw, C.E. (2008) TDP-43 mutations in familial and sporadic amyotrophic lateral sclerosis. Science 319, 1668–1672.

[7] Rutherford, N.J., Zhang, Y.J., Baker, M., Gass, J.M., Finch, N.A., Xu, Y.F., Stewart, H., Kelley, B.J., Kuntz, K., Crook, R.J., Sreedharan, J., Vance, C., Sorenson, E., Lippa, C., Bigio, E.H., Geschwind, D.H., Knopman, D.S., Mitsumoto, H., Petersen, R.C., Cashman, N.R., Hutton, M., Shaw, C.E., Boylan, K.B., Boeve, B., Graff-Radford, N.R., Wszolek, Z.K., Caselli, R.J., Dickson, D.W., Mackenzie, I.R., Petrucelli, L. and Rademakers, R. (2008) Novel mutations in TARDBP (TDP-43) in patients with familial amyotrophic lateral sclerosis. PLoS Genet. 4, e1000193.

[8] Kabashi, E., Valdmanis, P.N., Dion, P., Spiegelman, D., McConkey, B.J., Vande Velde, C., Bouchard, J.P., Lacomblez, L., Pochigaeva, K., Salachas, F., Pradat, P.F., Camu, W., Meininger, V., Dupre, N. and Rouleau, G.A. (2008) TARDBP mutations in individuals with sporadic and familial amyotrophic lateral sclerosis. Nat. Genet. 40, 572–574.

[9] Gitcho, M.A., Baloh, R.H., Chakraverty, S., Mayo, K., Norton, J.B., Levitch, D., Hatanpaa, K.J., White 3rd, C.L., Bigio, E.H., Caselli, R., Baker, M., Al-Lozi, M.T., Morris, J.C., Pestronk, A., Rademakers, R., Goate, A.M. and Cairns, N.J. (2008) TDP-43 A315T mutation in familial motor neuron disease. Ann. Neurol. 63, 535–538.

[10] Arai, T., Mackenzie, I.R., Hasegawa, M., Nonoka, T., Niizato, K., Tsuchiya, K., Iritani, S., Onaya, M. and Akiyama, H. (2009) Phosphorylated TDP-43 in Alzheimer's disease and dementia with Lewy bodies. Acta Neuropathol. 117, 125–136.

[11] Hasegawa, M., Arai, T., Akiyama, H., Nonaka, T., Mori, H., Hashimoto, T., Yamazaki, M. and Oyanagi, K. (2007) TDP-43 is deposited in the Guam parkinsonism-dementia complex brains. Brain 130, 1386–1394.

[12] Fujishiro, H., Uchikado, H., Arai, T., Hasegawa, M., Akiyama, H., Yokota, O., Tsuchiya, K., Togo, T., Iseki, E. and Hirayasu, Y. (2009) Accumulation of phosphorylated TDP-43 in brains of patients with argyrophilic grain disease. Acta Neuropathol. 117, 151–158.

[13] Schwab, C., Arai, T., Hasegawa, M., Yu, S. and McGeer, P.L. (2008) Colocalization of transactivation-responsive DNA-binding protein 43 and huntingtin in inclusions of huntington disease. J. Neuropathol. Exp. Neurol. 67, 1159–1165.

[14] Farrer, M.J., Hulihan, M.M., Kachergus, J.M., Dachsel, J.C., Stoessl, A.J., Grantier, L.L., Calne, S., Calne, D.B., Lechevalier, B., Chapon, F., Tsuboi, Y., Yamada, T., Gutmann, L., Elibol, B., Bhatia, K.P., Wider, C., Vilarino-Guell, C., Ross, O.A., Brown, L.A., Castanedes-Casey, M., Dickson, D.W. and Wszolek, Z.K. (2009) DCTN1 mutations in Perry syndrome. Nat. Genet. 41, 163–165.

[15] Schwab, C., Arai, T., Hasegawa, M., Akiyama, H., Yu, S. and McGeer, P.L. (2009) TDP-43 pathology in familial British dementia. Acta Neuropathol., in press, doi:10.1007/s00401-009-0514-3.

[16] Gura, T. (2008) Hope in Alzheimer's fight emerges from unexpected places. Nat. Med. 14, 894.

[17] Doody, R.S., Gavrilova, S.I., Sano, M., Thomas, R.G., Aisen, P.S., Bachurin, S.O., Seely, L. and Hung, D. (2008) Effect of dimebon on cognition, activities of daily living, behaviour, and global function in patients with mild-to-moderate Alzheimer's disease: a randomised, double-blind, placebo-controlled study. Lancet 372, 207–215.

[18] Kristiansen, J.E. (1989) Dyes, antipsychotic drugs, and antimicrobial activity. Fragments of a development, with special reference to the influence of Paul Ehrlich. Dan Med. Bull. 36, 178–185.

[19] Mansouri, A. and Lurie, A.A. (1993) Concise review: methemoglobinemia. Am. J. Hematol. 42, 7–12.

[20] Faber, P., Ronald, A. and Millar, B.W. (2005) Methylthioninium chloride: pharmacology and clinical applications with special emphasis on nitric oxide mediated vasodilatory shock during cardiopulmonary bypass. Anaesthesia 60, 575–587.

[21] Heiberg, I.L., Wegener, G. and Rosenberg, R. (2002) Reduction of cGMP and nitric oxide has antidepressant-like effects in the forced swimming test in rats. Behav. Brain Res. 134, 479–484.

[22] Visarius, T.M., Stucki, J.W. and Lauterburg, B.H. (1997) Stimulation of respiration by methylene blue in rat liver mitochondria. FEBS Lett. 412, 157–160.

[23] Chies, A.B., Custodio, R.C., de Souza, G.L., Correa, F.M. and Pereira, O.C. (2003) Pharmacological evidence that methylene blue inhibits noradrenaline neuronal uptake in the rat vas deferens. Pol. J. Pharmacol. 55, 573–579.

[24] Wrubel, K.M., Riha, P.D., Maldonado, M.A., McCollum, D. and Gonzalez-Lima, F. (2007) The brain metabolic enhancer methylene blue improves discrimination learning in rats. Pharmacol. Biochem. Behav. 86, 712–717.

[25] Atamna, H., Nguyen, A., Schultz, C., Boyle, K., Newberry, J., Kato, H. and Ames, B.N. (2008) Methylene blue delays cellular senescence and enhances key mitochondrial biochemical pathways. FASEB J. 22, 703–712.

[26] Wischik, C.M., Edwards, P.C., Lai, R.Y., Roth, M. and Harrington, C.R. (1996) Selective inhibition of Alzheimer disease-like tau aggregation by phenothiazines. Proc. Natl. Acad. Sci. USA 93, 11213–11218.

[27] Taniguchi, S., Suzuki, N., Masuda, M., Hisanaga, S., Iwatsubo, T., Goedert, M. and Hasegawa, M. (2005) Inhibition of heparin-induced tau filament formation by phenothiazines, polyphenols, and porphyrins. J. Biol. Chem. 280, 7614–7623.

[28] Burns, A. and Jacoby, R. (2008) Dimebon in Alzheimer's disease: old drug for new indication. Lancet 372, 179–180.

[29] Bachurin, S., Bukatina, E., Lermontova, N., Tkachenko, S., Afanasiev, A., Grigoriev, V., Grigorieva, I., Ivanov, Y., Sablin, S. and Zefirov, N. (2001) Antihistamine agent Dimebon as a novel neuroprotector and a cognition enhancer. Ann. NY Acad. Sci. 939, 425–435.

[30] Wu, J., Li, Q. and Bezprozvanny, I. (2008) Evaluation of dimebon in cellular model of Huntington's disease. Mol. Neurodegener. 3, 15.

[31] Lermontova, N.N., Redkozubov, A.E., Shevtsova, E.F., Serkova, T.P., Kireeva, E.G. and Bachurin, S.O. (2001) Dimebon and tacrine inhibit neurotoxic action of beta-amyloid in culture and block L-type Ca(2+) channels. Bull. Exp. Biol. Med. 132, 1079–1083.

[32] Bahurin, S.O., Ustyugov, A.A., Peters, O., Shelkovnikova, T.A., Buchman, V.L. and Ninkina, N.N. (2009). Hindering of proteinopathy-induced neurodegeneration as a new mechanism of action for neuroprotectors and cognition enhancing compounds. Dokl. Biochem. Biophys., in press.

[33] Nonaka, T., Arai, T., Buratti, E., Baralle, F.E., Akiyama, H. and Hasegawa, M. (2009) Phosphorylated and ubiquitinated TDP-43 pathological inclusions in ALS and FTLD-U are recapitulated in SH-SY5Y cells. FEBS Lett. 583, 394–400.

[34] Nonaka, T., Kametani, F., Arai, T., Akiyama, H. and Hasegawa, M. (2009). Truncation and pathogenic mutations facilitate the formation of intracellular aggregates of TDP-43. Hum. Mol. Genet., in press, doi:10.1093/hmg/ddp275.

[35] Johnson, B.S., McCaffery, J.M., Lindquist, S. and Gitler, A.D. (2008) A yeast TDP-43 proteinopathy model: exploring the molecular determinants of TDP-43 aggregation and cellular toxicity. Proc. Natl. Acad. Sci. USA 105, 6439–6444.

[36] Lermontova, N.N., Lukoyanov, N.V., Serkova, T.P., Lukoyanova, E.A. and Bachurin, S.O. (2000) Dimebon improves learning in animals with experimental Alzheimer's disease. Bull. Exp. Biol. Med. 129, 544–546.

[37] Tatom, J.B., Wang, D.B., Dayton, R.D., Skalli, O., Hutton, M.L., Dickson, D.W. and Klein, R.L. (2009) Mimicking aspects of frontotemporal lobar degeneration and Lou Gehrig's disease in rats via TDP-43 overexpression. Mol. Ther. 17, 607–613.

[38] Naylor, G.J., Martin, B., Hopwood, S.E. and Watson, Y. (1986) A two-year double-blind crossover trial of the prophylactic effect of methylene blue in manic-depressive psychosis. Biol. Psychiatr. 21, 915–920.

[39] Sills, M.R. and Zinkham, W.H. (1994) Methylene blue-induced Heinz body hemolytic anemia. Arch Pediatr. Adolesc. Med. 148, 306–310.

Human Molecular Genetics, 2009, Vol. 18, No. 18 *3353–3364*
doi:10.1093/hmg/ddp275
Advance Access published on June 10, 2009

Truncation and pathogenic mutations facilitate the formation of intracellular aggregates of TDP-43

Takashi Nonaka[1,*], Fuyuki Kametani[1], Tetsuaki Arai[2], Haruhiko Akiyama[2] and Masato Hasegawa[1,*]

[1]Department of Molecular Neurobiology and [2]Department of Psychogeriatrics, Tokyo Institute of Psychiatry, Tokyo Metropolitan Organization for Medical Research, 2-1-8 Kamikitazawa, Setagaya-ku, Tokyo 156-8585, Japan

Received April 5, 2009; Revised May 27, 2009; Accepted June 8, 2009

TAR DNA binding protein of 43 kDa (TDP-43) is a major component of the ubiquitin-positive inclusions found in the brain of patients with frontotemporal lobar degeneration (FTLD-U) and amyotrophic lateral sclerosis (ALS). Here, we report that expression of TDP-43 C-terminal fragments as green fluorescent protein (GFP) fusions in SH-SY5Y cells results in the formation of abnormally phosphorylated and ubiquitinated inclusions that are similar to those found in FTLD-U and ALS. Co-expression of DsRed-tagged full-length TDP-43 with GFP-tagged C-terminal fragments of TDP-43 causes formation of cytoplasmic inclusions positive for both GFP and DsRed. Cells with GFP and DsRed positive inclusions lack normal nuclear staining for endogenous TDP-43. These results suggest that GFP-tagged C-terminal fragments of TDP-43 are bound not only to transfected DsRed-full-length TDP-43 but also to endogenous TDP-43. Endogenous TDP-43 may be recruited to cytoplasmic aggregates of TDP-43 C-terminal fragments, which results in the failure of its nuclear localization and function. Interestingly, expression of GFP-tagged TDP-43 C-terminal fragments harboring pathogenic mutations that cause ALS significantly enhances the formation of inclusions. We also identified cleavage sites of TDP-43 C-terminal fragments deposited in the FTLD-U brains using mass spectrometric analyses. We propose that generation and aggregation of phosphorylated C-terminal fragments of TDP-43 play a primary role in the formation of inclusions and resultant loss of normal TDP-43 localization, leading to neuronal degeneration in TDP-43 proteinopathy.

INTRODUCTION

Progressive neuronal loss and abnormal protein deposits as intracellular inclusions are neuropathological features of the majority of neurodegenerative disorders, as exemplified by tau in Alzheimer's disease (AD), alpha-synuclein in Parkinson's disease (PD) and expanded polyglutamine gene products in CAG repeat diseases. Conformational changes, post-translational modifications or subcellular mislocalization of these normally highly soluble proteins results in the formation of abnormal protein aggregates or inclusions. It is important to establish the molecular mechanisms through which these proteins are converted to abnormal aggregates in neurons or glial cells in order to understand the pathogenesis of these diseases and to develop evidence-based, fundamental therapies.

Frontotemporal lobar degeneration with ubiquitinated inclusions (FTLD-U) and amyotrophic lateral sclerosis (ALS) are well-known neurodegenerative disorders. FTLD is the second most common form of cortical dementia in the population below the age of 65 years (1). ALS is the most common of the motor neuron diseases, being characterized by progressive weakness and muscular wasting, resulting in death within a few years. Ubiquitin (Ub)-positive inclusions are found as a pathological hallmark in brains of FTLD-U and ALS patients, as well as in AD and PD, but the major component of these inclusions had remained unknown. TAR-DNA binding protein of 43 kDa (TDP-43) has been identified as a major protein component of Ub-positive inclusions in FTLD-U and ALS brains (2,3). In 2008, mutations in the TDP-43 gene were discovered in familial

*To whom correspondence should be addressed. Tel: +81 333045701; Fax: +81 333298035; Email: nonakat@prit.go.jp (T.N.)/masato@prit.go.jp (M.H.)

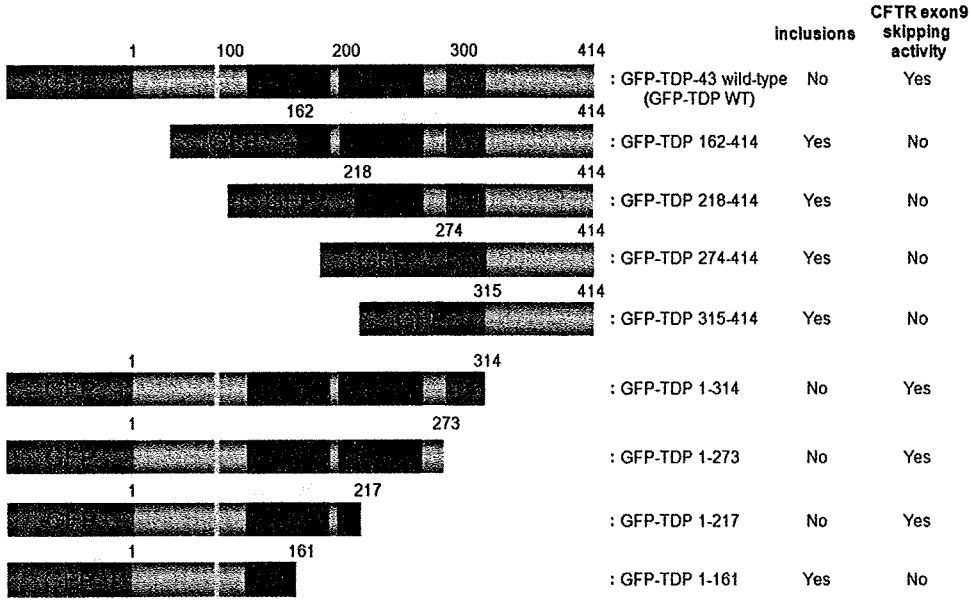

Figure 1. Schematic diagram of GFP-tagged N-terminal and C-terminal TDP-43 fragments. Green fluorescent protein (GFP), nuclear localization signal (NLS: 82–98 residues), two RNA-recognition motifs (RRM-1, 105–169 residues; RRM-2, 193–257 residues) and glycine-rich domain (274–314 residues) were colored green, yellow, blue and red, respectively. The formation of inclusions and the exon skipping ability of each fragment were reported on the right. The CFTR exon 9 skipping activity of these fragments were determined as shown in Fig. 5.

and sporadic cases of ALS (4–8), clearly indicating that abnormality of TDP-43 protein causes neurodegeneration. Very recently, it was also reported that two TDP-43 mutations were found in FTLD-MND patients (9). In previous genetic studies of familial ALS, superoxide dismutase 1 (SOD1) gene mutation was considered to be responsible for ~20% of cases (10,11). It has been reported, however, that TDP-43 is not deposited in spinal cords of familial ALS patients with SOD1 mutations (12,13). These observations suggest that the mechanisms of motor neuron degeneration caused by SOD1 mutations are different from those in sporadic ALS. TDP-43 is also a major component of skein-like inclusions seen in 100% of sporadic ALS cases (14). Thus, it is important to investigate the molecular mechanisms of TDP-43-mediated neurodegeneration in order to understand the pathogenesis and to develop effective treatments for sporadic ALS and other TDP-43 proteinopathies. One of the known biochemical features of TDP-43 deposited in FTLD-U and ALS brains is the presence of truncated TDP-43 fragments (2,3). Recently, using multiple anti-phosphorylated TDP-43 specific antibodies including pS409/410-specific antibodies, we have shown that 18–26 kDa C-terminal fragments of TDP-43 are major constituents of inclusions in FTLD-U and ALS brains (15).

In this study, we investigated the roles of fragmentation and pathogenic mutations of TDP-43 for the formation of Ub-positive inclusions in SH-SY5Y cells. Here we show that expression of TDP-43 C-terminal fragments results in the formation of cytoplasmic inclusions positive for antibodies to phosphorylated TDP-43 and Ub, and incorporation of newly synthesized endogenous full-length TDP-43 into cytoplasmic aggregates of the C-terminal fragments. Expression of fourteen pathogenic ALS mutations so far discovered in the TDP-43 gene shows a propensity to promote intracellular aggregation. Furthermore, using mass spectrometric analysis, we have successfully identified new cleavage sites of C-terminal fragments of TDP-43 deposited in FTLD-U brains.

RESULTS

Expression of TDP-43 fragments in SH-SY5Y cells

To examine whether C-terminal fragments of TDP-43 readily aggregate in neuronal cells, we expressed several kinds of N-terminal and C-terminal fragments of TDP-43 and full-length TDP-43 as GFP-fusions (Fig. 1). Confocal microscopic analysis showed that the fluorescence of GFP-tagged full-length TDP-43 (GFP-TDP WT) was mainly localized in the nuclei (Fig. 2B). This is consistent with the expression pattern of non-tagged wild-type TDP-43 (16), suggesting that the GFP tag did not alter the cellular localization of TDP-43.

When cells were transfected with GFP-TDP 162-414 or GFP-TDP 218-414, round or dot-like cytoplasmic structures with intense GFP fluorescence were found (Fig. 2C–F). These structures were positive for both anti-pS409/410 and anti-Ub antibodies (Fig. 2C–F). Cells expressing GFP-TDP 274–414 (Fig. 2G and H) and GFP-TDP 315–414 (Fig. 2I and J), on the other hand, showed diffuse GFP staining and pS409/410-positive but Ub-negative inclusion-like structures. We previously reported the presence of such pS409/410-positive and Ub-negative inclusions in the brains of FTLD-U and ALS cases (15). The expression of these all C-terminal fragments was found in cytoplasm by analyses using confocal microscopy (Fig. 2) and biochemical fractionation (Supplementary Material, Fig. S1A), because they lacks nuclear localization signal (16,17). Taken together, these results indicate that cytoplasmic expression of C-terminal

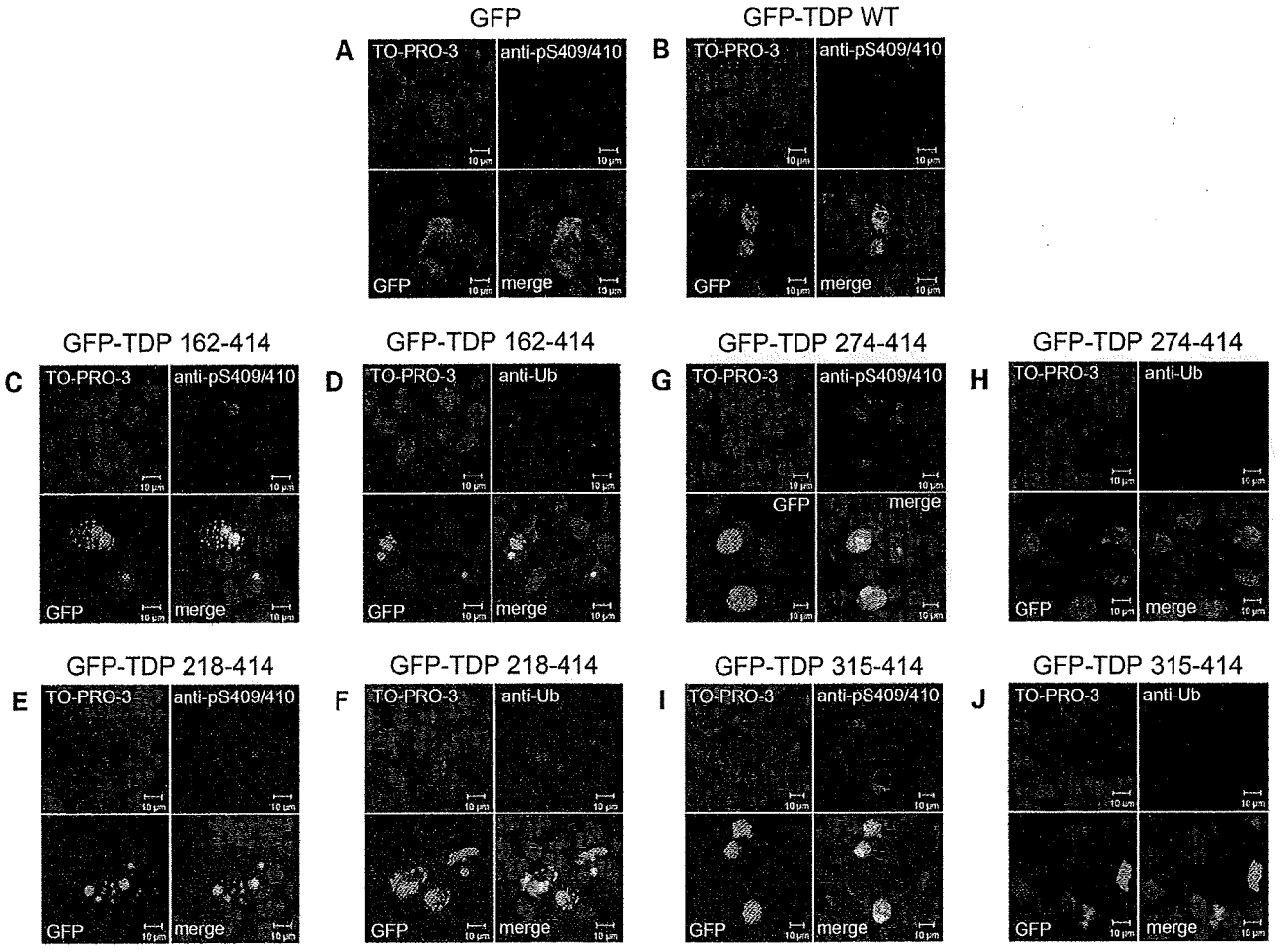

Figure 2. Expression of GFP-tagged C-terminal fragments of TDP-43 leads to aggregate formation in SH-SY5Y cells. SH-SY5Y cells 72 h post-transfection with GFP (**A**), GFP-tagged TDP-43 wild-type (GFP-TDP WT) (**B**), GFP-tagged fragments of residues 162–414 (GFP-TDP 162–414) (**C** and **D**), GFP-TDP 218–414 (**E** and **F**), GFP-TDP 274–414 (**G** and **H**) and GFP-TDP 315–414 (**I** and **J**) were stained with anti-pS409/410 (A, B, C, E, G, I) or anti-Ub (D, F, H, J). DNA was labeled with TO-PRO-3. Note that there are intracellular inclusion-like structures positive for both anti-Ub and anti-pS409/410 antibodies in cells expressing GFP-TDP 162–414 (C, D) and GFP-TDP 218–414 (E, F).

fragments of TDP-43 results in the formation of intracellular aggregates similar to those found in diseased brains.

N-terminal fragments of GFP-TDP-43 were also expressed in SH-SY5Y cells and analyzed using confocal microscopy and biochemical fractionation. As shown in Fig. 3A, irregularly shaped cytoplasmic structures with strong GFP fluorescence, which are partially positive for Ub, were observed in cells expressing GFP-TDP 1–161. Only a few aggregates positive for Ub were observed in cells transfected with GFP-TDP 1–217 (Fig. 3B). Since these fragments lack the epitope for anti-pS409/410, the phosphorylation state of these structures could not be determined by immunohistochemistry. None of the cells transfected with other N-terminal fragments had any Ub-positive inclusion-like structures (Fig. 3C and D). The results of biochemical fractionation showed that the amount of these N-terminal fragments was greater in the cytoplasm than in the nucleus, while that of GFP-TDP WT was greater in the nucleus than in the cytoplasm (Supplementary Material, Fig. S1A). These results suggest that truncations of TDP-43 C-terminal regions affect normal targeting of TDP-43 to nuclei. This observation is in good agreement with the previous report by Ayala *et al.* (18).

Since intracellular inclusion-like structures showed the highest-intensity GFP signals in Figs 2 and 3, they were able to be selectively detected by reducing the laser power at 488 nm. Quantitative analyses under such analytical conditions clearly indicated that significantly a larger number of intracellular aggregates were formed in cells expressing GFP-TDP 162–414, GFP-TDP 218–414 and GFP-TDP 1–161 than in cells expressing GFP-TDP WT (Fig. 3E).

Figure 4 shows the results of immunoblot analyses of cell lysates using anti-GFP, a commercially available phosphorylation-independent anti-TDP-43 (ProteinTech), and anti-pS409/410 antibodies. Anti-TDP-43 detected endogenous TDP-43 at 43 kDa, exogenous full-length TDP-43, all N-terminal fragments and GFP-TDP 162–414, but did not GFP-TDP 218–414, 274–414 and 315–414 (Fig. 4A and D). These results suggest that the epitopes of this antibody are located in the N-terminal region between 1 and 217 residues. Anti-GFP antibody stained all the exogenous TDP-43

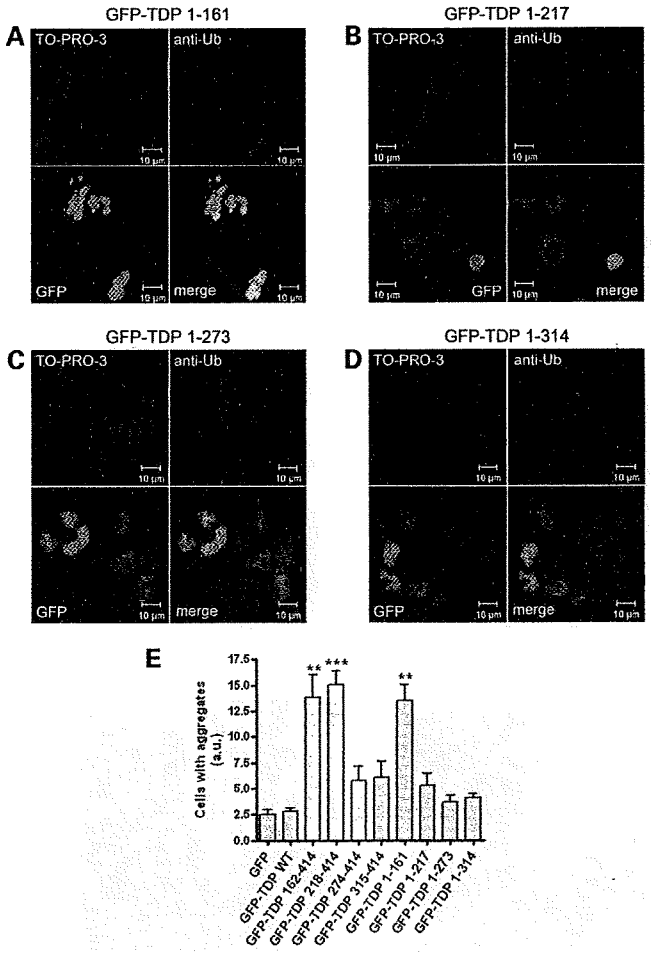

Figure 3. Expression of GFP-tagged N-terminal fragments of TDP-43 resulted in the formation of intracellular inclusions in SH-SY5Y cells. SH-SY5Y cells 72 h post-transfection with GFP-tagged fragments of 1–161 residues (GFP-TDP 1–161) (**A**), GFP-TDP 1–217 (**B**), GFP-TDP 1–273 (**C**) and GFP-TDP 1–314 (**D**) were stained with anti-Ub. DNA was labeled with TO-PRO-3. Note the characteristic inclusions detected with anti-Ub antibody in cells transfected with GFP-TDP 1–161. (**E**) The rates of cells including intracellular aggregates were calculated in arbitrary units. Fluorescence intensity within an area of ~800 × 800 μm was assessed by confocal microscopy. The intensity of GFP was calculated as a ratio to that of TO-PRO-3. Six areas per sample were measured ($n = 6$). Data are means ± SEM. $^{**}P < 0.01$; $^{***}P < 0.001$ by Student's *t*-test against the value of GFP-TDP WT.

(Fig. 4B and E). In these immunoblot analyses, we used the intensity of the bands of endogenous TDP-43 (arrows in Fig. 4A and D) as a loading control. While the amounts of exogenous protein are nearly constant, that of 1–161 is relatively low and those of 274–414 and 315–414 relatively high. Nevertheless, such variability does not affect the occurrence or absence of inclusion formation (Fig. 1). Endogenous and exogenous full-length TDP-43 (GFP-TDP WT) were detected mostly in TS-, TX- and Sar-soluble fractions, and were negative for anti-pS409/410 (Fig. 4).

Although GFP-TDP 162–414 was also detected in TS-, TX- and Sar-soluble fractions with anti-TDP-43 and anti-GFP, a slightly higher-molecular-weight band (~60 kDa, black arrowhead in Fig. 4C) was detected in Sar-soluble and insoluble fractions with anti-pS409/410. A similar band was only weakly detected with anti-TDP-43 (black arrowhead in Fig. 4A), and was negative to anti-GFP antibody. These results confirmed our previous reports that our anti-pS409/410 is specific to and is more sensitive in detecting abnormally accumulated TDP-43 than phosphorylation-independent antibodies such as anti-TDP-43 (ProteinTech) (15,16,19). Anti-GFP used here seems to be less sensitive in immunoblot. Anti-GFP may also be affected by possible structural changes during aggregates formation when applied to the Sarkosyl insoluble fraction. GFP-TDP 218–414 was mainly detected in Sar-soluble and -insoluble fractions with anti-GFP (Fig. 4B), and a slightly higher-molecular-weight band at 52 kDa (white arrowhead in Fig. 4C) and smears were visualized in the Sar-soluble and -insoluble fractions with anti-pS409/410. Similarly, pS409/410-positive bands were detected in the Sar-soluble and insoluble fractions of cell lysates expressing GFP-TDP 274–414 or GFP-TDP 315–414 (black-lined arrowhead for GFP-TDP-274–414; white-lined arrowhead for GFP-TDP 315–414 in Fig. 4C), although no abnormal band pattern was detected with anti-TDP-43 or anti-GFP.

The N-terminal fragments, including GFP-TDP 1–314, GFP-TDP 1–273 and GFP-TDP 1–217, were detected mainly in the TS- and TX-soluble fractions, together with GFP-TDP WT and endogenous TDP-43 (Fig. 4D and E). However, GFP-TDP 1–161, the shortest N-terminal fragment, was detected only in the Sar-soluble fraction (black-lined arrowheads in Fig. 4D and E), which is consistent with the inclusion formation observed in cells expressing this fragment, as shown in Fig. 3A.

Loss of function and intracellular accumulation of TDP-43 fragments

TDP-43 has been reported to regulate the alternative splicing of exon 9 of cystic fibrosis transmembrane conductance regulator (CFTR) transcripts (20). TDP-43 is capable of binding to a (UG)nUm element in CFTR intron 8 near its junction with exon 9. Through this binding, TDP-43 enhances the exon skipping of exon 9 during CFTR splicing. To evaluate the functional significance of TDP-43 fragments used in this study, we performed CFTR exon 9 skipping assay (16). We co-transfected the expression plasmid of TDP-43 wild-type or fragments with the reporter plasmid pSPL3-CFTR9 (including a TG11T7 polymorphic locus) (16) into SH-SY5Y cells. The transcripts with and without the CFTR exon 9 insert are expected to be 360 and 177 bp long, respectively (16), and these were analyzed by RT–PCR. As shown in Fig. 5, mRNA from cells transfected with empty vector pEGFP gave only one RT–PCR band of 360 bp, while that from cells transfected with TDP-43 wild-type gave two RT–PCR bands, 360 and 177 bp, showing that skipping of CFTR exon 9 was increased by expression of GFP-TDP WT. We also confirmed that the GFP portion did not affect the CFTR exon skipping activity of TDP-43. All mRNAs from cells co-transfected with the C-terminal fragments showed one RT–PCR band of 360 bp (Fig. 5A). Of the four mRNAs from cells co-transfected with the N-terminal fragments, mRNA from GFP-TDP 1-161 showed a band of 360 bp, while the others showed two bands of 360 and 177 bp (Fig. 5B). These results indicate that the fragments without

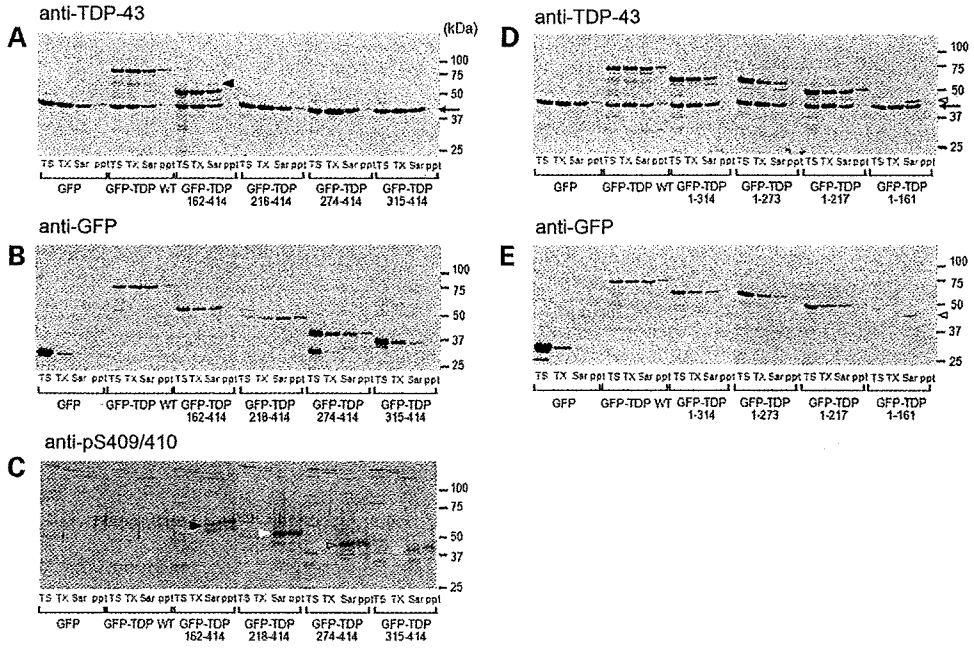

Figure 4. Immunoblot analyses of inclusions composed of GFP-tagged N-terminal and C-terminal fragments of TDP-43. SH-SY5Y cells, 72 h post-transfection with GFP alone or GFP-fused TDP-43 fragments, were sequentially extracted with Tris-saline (TS), 1% Triton X-100 (TX) and 1% Sarkosyl (Sar), and the supernatants and the Sarkosyl-insoluble pellets (ppt) were subjected to SDS–PAGE. Bands were transferred to PVDF membrane and probed with anti-TDP-43 antibody (**A** and **D**), anti-GFP antibody (**B** and **E**) and anti-pS409/410 antibody (**C**). The arrow indicated the band of endogenous TDP-43. Note that bands of pS409/410-positive C-terminal fragments were detected in Sarkosyl-soluble or -insoluble fractions of cells expressing GFP-TDP 162–414 (black arrowhead in C), GFP-TDP 218–414 (white arrowhead in C), GFP-TDP 274–414 (black-lined arrowhead in C) and GFP-TDP 315–414 (white-lined arrowhead in C), and that N-terminal fragment of GFP-TDP 1–161 was recovered in TX-insoluble fractions (black-lined arrowhead in D and E).

the entire RRM-1 motif do not have exon skipping activity, while the wild-type and fragments with the RRM-1 motif have the activity (Figs 1 and 5). These results are in good agreement with the observation by Buratti and Baralle (21) that the RRM-1 domain is necessary for binding with RNA. It is noteworthy that all the TDP-43 fragments which form intracellular aggregates lack exon skipping activity.

Expression of TDP-43 C-terminal fragment facilitates aggregation of full-length TDP-43 in SH-SY5Y cells

To test whether C-terminal fragments of TDP-43 interact with full-length TDP-43, C-terminal fragments of GFP-TDP-43 or full-length GFP-TDP-43 was co-expressed with full-length DsRed-fused TDP-43 (DsRed-TDP-43) in SH-SY5Y cells. Immunoprecipitation experiments of cell lysates using agarose conjugated anti-GFP followed by immunoblotting with anti-RFP or anti-TDP-43 showed that GFP-TDP-43 C-terminal fragments as well as full-length GFP-TDP-43 were bound to full-length DsRed-TDP-43 (Fig. 6). Full-length GFP-TDP-43 was found to more strongly interact with DsRed-TDP-43 than any other C-terminal fragments of GFP-TDP-43. The experiments also showed a weak but notable interaction between endogenous TDP-43 and full-length GFP-TDP-43 or C-terminal fragments of GFP-TDP-43. These results suggest that both full-length GFP-TDP-43 and its C-terminal fragments interact not only with full-length DsRed-TDP-43 but also with endogenous TDP-43 in SH-SY5Y cells.

To monitor the intracellular interaction between endogenous TDP-43 and C-terminal fragments of GFP-TDP-43, SH-SY5Y cells were transfected with GFP-TDP 162–414 or GFP-TDP 218–414 and analyzed by confocal microscopy. Immunostaining using anti-TDP-43 showed that full-length GFP-TDP-43 was co-localized with endogenous TDP-43 in nuclei (Fig. 7A). We observed that GFP signals from cytoplasmic inclusions of GFP-TDP 162–414 or GFP-TDP 218–414 were overlapped with immunoreactivities of anti-TDP-43. Furthermore, immunoreactivities of anti-TDP-43 were almost eliminated from the nuclei of these cells (Fig. 7B and C). When full-length GFP-TDP-43 was co-expressed with full-length DsRed-TDP-43, both proteins were found to be localized in nuclei with no formation of inclusion-like structures (Fig. 7D). In contrast, round cytoplasmic inclusions with both GFP and DsRed signals appeared when GFP-TDP 162–414 (Fig. 7E) or GFP-TDP 218–414 (Fig. 7F) was co-expressed with full-length DsRed-TDP-43. These results indicate that endogenous TDP-43 or exogenous full-length DsRed-TDP-43 is trapped into cytoplasmic inclusions formed by GFP-TDP 162–414 or GFP-TDP 218–414, which is consistent with the results of immunoprecipitation experiments shown in Fig. 6.

Effects of pathogenic mutations on aggregation of TDP-43

Then, we tested the effect of mutations of the TDP-43 gene found in familial and sporadic ALS cases on the intracellular aggregates of C-terminal fragments of GFP-TDP-43 (GFP-TDP 162–414). GFP-TDP 162–414 with or without mutations was expressed in SH-SY5Y cells, which were then analyzed by immunoblot and confocal microscopy. We first confirmed almost same expression levels of all exogenous

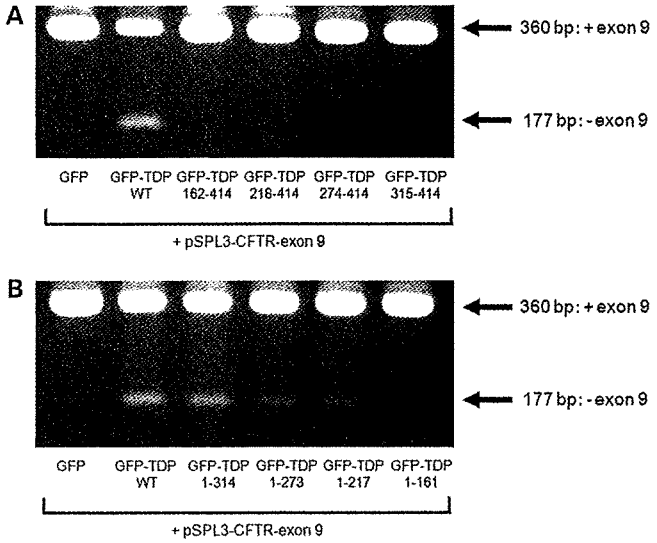

Figure 5. CFTR exon 9 skipping assay of GFP-tagged TDP-43 fragments. (**A** and **B**) Gel electrophoresis of RT–PCR products of RNA from transfected cos-7 cells. The RNAs from cos-7 cells, co-transfected with the reporter plasmid pSPL3-CFTR exon 9 (TG11T7) plus pEGFP-TDP-43 expression vectors, were used as templates for RT–PCR analysis. The products were analyzed by electrophoresis in 1.5% agarose gel.

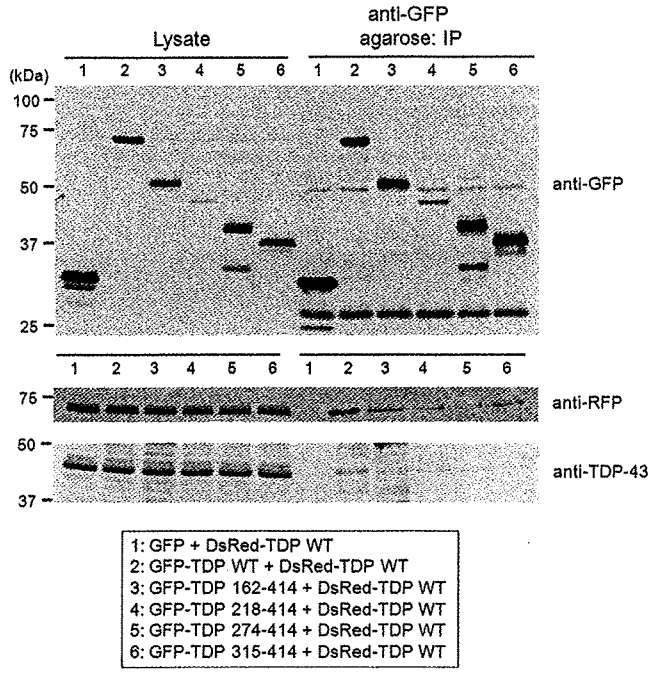

Figure 6. Full-length GFP-TDP-43 and its C-terminal fragments interact not only with full-length DsRed-TDP-43 but also with endogenous TDP-43. SH-SY5Y cells were transfected with pDsRed-TDP-43 wild-type (DsRed-TDP WT) and pEGFP-C1 (GFP; lane 1), pEGFP-TDP-43 WT (GFP-TDP WT; lane 2), pEGFP-TDP 162–414 (GFP-TDP 162–414; lane 3), pEGFP-TDP 218–414 (GFP-TDP 218–414; lane 4), pEGFP-TDP 274–414 (GFP-TDP 274–414; lane 5) or pEGFP-TDP 315–414 (GFP-TDP 315–414; lane 6), for 3 days, and analyzed by immunoprecipitation. Cell lysates (total protein: ~100 μg) was recovered and subjected to IP with agarose conjugated anti-GFP (~5 μg of anti-GFP, MBL). Bounds proteins were eluted from the beads with SDS sample buffer. Each sample (~5 μg of lysates and ~1/5 aliquots of IP fraction) was separated by 10% SDS–PAGE and immunoblotted with anti-GFP antibody, anti-RFP antibody and anti-TDP-43 antibody.

GFP-TDP 162–414 with or without mutations by immunoblot analysis with anti-TDP-43 (Fig. S2). Figure 8 showed that all 14 mutant GFP-TDP 162–414 formed more intracellular aggregates than wild-type GFP-TDP 162–414. Of these mutations, the number of cells with aggregates was significantly higher in GFP-TDP 162–414 with D169G, G294A, Q331K, M337V, Q343R, N390D and N390S, when compared with the wild-type GFP-TDP 162–414 (Fig. 8B).

When full-length TDP-43 with or without GFP fusion was expressed in cells, we could not find any significant difference in the number of cells with aggregates between wild-type and all mutants (data not shown). Furthermore, there was no significant difference in the generation of TDP-43 fragments (Supplementary Material, Fig. S3) or exon skipping activity of CFTR exon 9 between wild-type full-length TDP-43 and mutated full-length TDP-43 (data not shown).

Identification of the cleavage sites of N-terminally truncated TDP-43 fragments in FTLD-U brains

To identify the cleavage sites of the C-terminal fragments of TDP-43 accumulated in brains of FTLD-U patients, we performed protein chemical analyses of the major fragments of 18–26 kDa in the Sarkosyl-insoluble fraction (Fig. 9A). Mass spectra analysis of tryptic digests of these fragments identified two typical tryptic peptides, (K)GISVHISNAEPKHNSNR (residues 252–268) and (R)FGGNPGGFG NQGGFGNSR (residues 276–293), and two unusual tryptic peptides, (M)DVFIPKPFR (residues 219–227) (Fig. 9B) and (E)DLIIK (residues 247–251) (Fig. 9C). N-termini of the latter two peptides are not produced by trypsin, because this enzyme cannot cleave Met218-Asp219 and Glu246-Asp247 bonds. These results suggest that these peptides are N-terminal parts of C-terminal fragments of TDP-43, and that the major C-terminal fragments deposited in FTLD-U brains are produced by cleavage between Met218-Asp219 or Glu246-Asp247.

To characterize these C-terminal fragments of TDP-43 deposited in FTLD-U brains with regards to intracellular aggregates formation, phosphorylation, and CFTR exon 9 splicing activity, GFP-TDP 219–414 and GFP-TDP 247–414 were constructed and expressed in SH-SY5Y cells for 3 days. These cells were analyzed using confocal microscopy, immunoblot and CFTR exon 9 skipping assay. As shown in Fig. 10A, round cytoplasmic inclusions with GFP fluorescence were clearly observed in cells expressing GFP-TDP 219–414 or GFP-TDP 247–414. These were also positive for anti-pS409/410 and anti-Ub. In immunoblot analyses, GFP-TDP 219–414 and GFP-TDP 247–414 were detected in Sar-soluble and insoluble fractions with anti-pS409/410 (Fig. 10B). These results suggest that these C-terminal fragments have high propensity to aggregate in cells, which is in good agreement with above results obtained from cells expressing other C-terminal fragments (e.g. GFP-TDP 218–414). Furthermore, expression of each C-terminal fragment resulted in a decrease in exon 9 skipping activity relative to GFP-TDP wild-type, as shown in Fig. 10C. We also found that overexpression of these C-terminal fragments led to a slight but

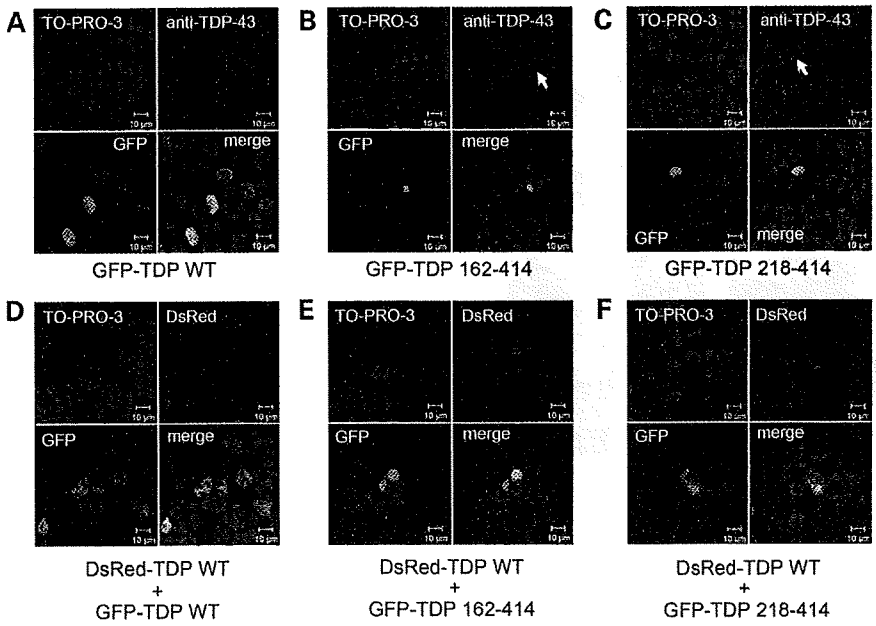

Figure 7. Co-expression of both DsRed-TDP-43 wild-type and GFP-TDP-43 wild-type or its C-terminal fragments. SH-SY5Y cells were transfected with pEGFP-TDP-43 wild-type (GFP-TDP WT), pEGFP-TDP 162–414 (GFP-TDP 162–414), pEGFP-TDP 218–414 (GFP-TDP 218–414) with (**D**–**F**) or without pDsRed-TDP-43 WT (**A**–**C**) for 3 days, and analyzed by confocal microscopy. Endogenous TDP-43 was stained by anti-TDP-43 antibody (ProteinTech) in (A–C). DNA was stained with TO-PRO-3. The threshold gain level of laser power (543 nm for detection of DsRed) was adjusted so that the signals did not overlap. Immunoreactivities of anti-TDP-43 were almost eliminated from the nuclei of cells with inclusions of GFP-TDP 162–414 (arrow in B) and GFP-TDP 218–414 (arrow in C).

significant increase in CFTR exon 9 inclusion (Fig. 10C, lower panel). This result suggests that endogenous TDP-43 was trapped with these aberrant C-terminal fragments, resulting a loss of exon 9 exclusion activity by endogenous TDP-43.

DISCUSSION

In this work, we showed that expression of C-terminal and N-terminal fragments of TDP-43 as GFP fusions resulted in the formation of phosphorylated and ubiquitinated aggregates in cultured cells. We first tried to express non-tagged C-terminal TDP-43 fragment (residues 162–414 or 218–414) in SH-SY5Y cells, but without success (data not shown). We then constructed plasmids encoding GFP-tagged N-terminal and C-terminal fragments of TDP-43, as shown in Fig. 1. The C-terminal fragments were significantly more prone to aggregate than full-length TDP-43. These aggregated C-terminal fragments were phosphorylated at Ser409 and Ser410, and were recovered in the TX-insoluble and Sar-soluble as well as Sar-insoluble fractions. These features are consistent with our previous findings, which showed that phosphorylated C-terminal fragments of TDP-43 were the major component of Sar-insoluble TDP-43 in the FTLD-U and ALS brains (15).

Recently, Johnson *et al.* (22) reported a yeast TDP-43 proteinopathy model. They found that RRM-2 and a C-terminal region (188–414 residues) are required for TDP-43 to form toxic aggregates. The fact that the highest propensity to aggregate was seen with GFP-TDP 162–414 and GFP-TDP 218–414 in the present study is consistent with their observations. However, the formation of pS409/410-positive inclusion-like structures in cells expressing C-terminal fragments without RRM2 (GFP-TDP 274–414 and 315–414), and the lack of striking cell death in cells expressing any GFP-tagged TDP-43 fragments (data not shown), differ from their findings. Furthermore, we could not detect intracellular aggregates formed by full-length GFP-TDP-43 in this study. One of the reasons for such discrepancies may be the differences between cultured neuronal cells and yeast.

We also found that one of the N-terminal fragments of TDP-43, GFP-TDP 1-161 were also prone to aggregate in cultured cells. This fragment was recovered in the TX-insoluble and Sar-soluble fraction. Previous reports indicated that lower-molecular-weight bands were present in the Sar-insoluble fractions of FTLD-U cases using the anti-TDP-43 (ProteinTech) (2,3,23). In this study, we established that this antibody recognizes the epitopes in the N-terminal portion between the residues 1 and 217 but not the C-terminal portion. Therefore, N-terminal fragments of TDP-43 may be present in the Sar-insoluble fraction of FTLD-U samples. It is noteworthy, therefore, that the expression of N-terminal TDP-43 fragments, as well as C-terminal fragments, could cause the formation of cytoplasmic aggregates in cultured cells.

The results of co-expression experiments using GFP-TDP 162–414 or GFP-TDP 218–414 and full-length DsRed-TDP-43 (Fig. 7) are consistent with the notion that cytoplasmic aggregates of C-terminal fragments of TDP-43 initially formed recruit newly synthesized full-length TDP-43 monomer and stay it in cytoplasm, resulting in depleting normal nuclear TDP-43. This may explain why normal TDP-43 staining is cleared in nuclei of diseased neurons containing cytoplasmic TDP-43 aggregates. Such mislocalization of full-length TDP-43 may induce neuronal dysfunction due to loss of

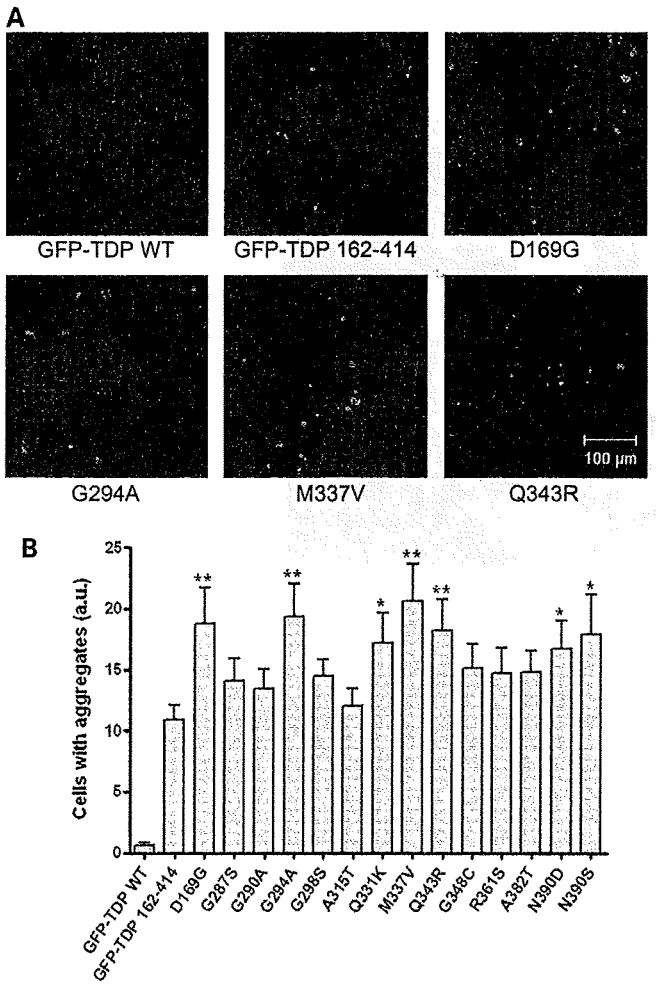

Figure 8. The effects of pathogenic mutations found in familial and sporadic ALS on intracellular accumulations of GFP-tagged TDP-43 C-terminal fragment. SH-SY5Y cells were transfected with GFP-TDP-43 wild-type (GFP-TDP WT), GFP-TDP 162-414 or each of 14 mutants (D169G, G287S, G290A, G294A, G298S, A315T, Q331K, M337V, Q343R, G348C, R361S, A382T, N390D and N390S) for 3 days, fixed and analyzed by confocal microscopy. DNA was stained with TO-PRO-3. (**A**) Images from cells transfected with GFP-TDP WT, GFP-TDP 162–414, GFP-TDP 162–414 with D169G (D169G), G294A (G294A), M337V (M337V) and Q343R (Q343R) were shown. (**B**) The rates of cells including intracellular aggregates were calculated in arbitrary units. Fluorescence intensity within an area of ~800 × 800 μm was assessed by confocal microscopy. The intensity of GFP was calculated as a ratio to that of TO-PRO-3. More than eight areas per sample were measured ($n = 8–16$). Data are means ± SEM. $^{*}P < 0.05$; $^{**}P < 0.01$ by Student's t-test against the value of GFP-TDP 162–414.

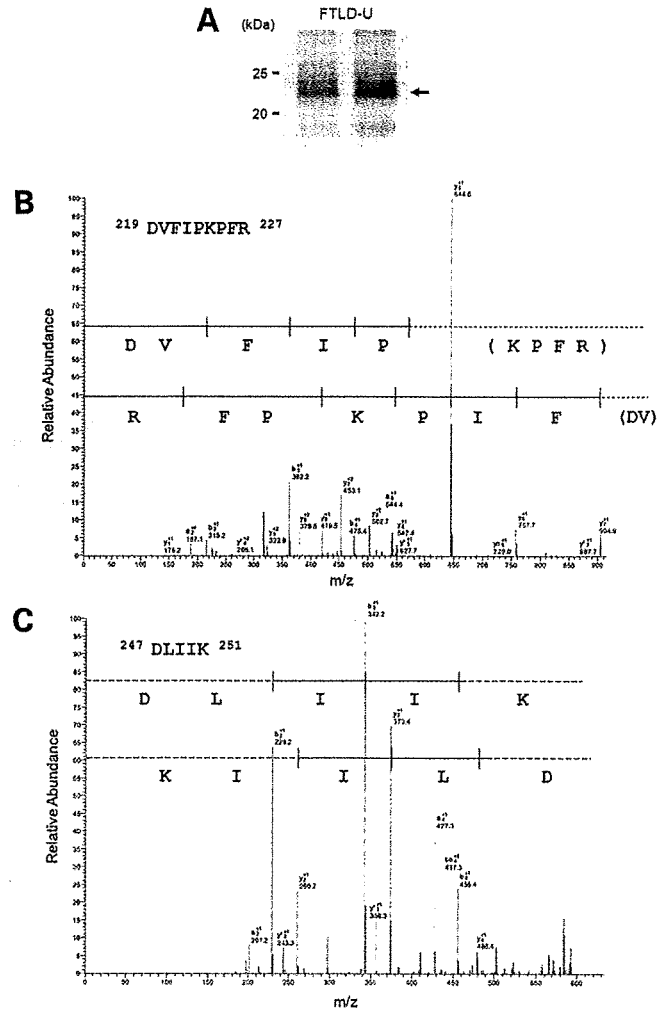

Figure 9. Identification of the cleavage site of TDP-43 C-terminal fragments deposited in FTLD-U brains. (**A**) C-terminal fragments of TDP-43 deposited in FTLD-U brains were detected with anti-pS409/410 (15). The pS409/410-positive ~23 kDa bands (an arrow) were dissected and digested in-gel with trypsin. (**B** and **C**) Product ion spectra of a mass signal $(M+2H)^{2+}$ of m/z 560.55 (B) and m/z 601.71 (C) from tryptic digests of urea-soluble C-terminal fragment of TDP-43 from FTLD-U brains. These spectra show the b and y ion series, identifying the peptide, DVFIPKPFR (residues 219–227) and DLIIK (residues 247–251), respectively. Vertical bars denote consecutive mass signals in b and y series.

physiological functions of TDP-43 in nuclei (3,17). In this study, we showed that expression of aberrant C-terminal fragment (GFP-TDP 219–414 or 247–414) resulted in decreased activity of CFTR exon 9 exclusion by endogenous TDP-43 due to its mislocalization in cytoplasm. It is also noteworthy that exogenously expressed full-length TDP-43 binds to each other, and the interaction between full-length TDP-43 is stronger than that between C-terminal fragments and full-length TDP-43. These results suggest that N-terminal portion may be essential for an inter-TDP-43 binding, which may contribute to its structural stability.

Interestingly, all TDP-43 fragments which form cytoplasmic aggregates lack CFTR exon 9 skipping activity (Figs 1 and 5). It was reported that the entire RRM-1 domain and C-terminal glycine-rich domain are required for CFTR exon 9 skipping (21,24–26). TDP-43 is considered to bind to hnRNP A/B through this domain (24). In our hands, all C-terminal fragments in this study lack skipping activity of CFTR exon 9, although these fragments retain the glycin-rich domain. Absence of RRM-1 or formation of cytoplasmic aggregates or both might impair the physiological functions of TDP-43, leading to cellular dysfunction and neurodegeneration. Further studies are needed to examine whether or not cellular function(s) (proliferation, differentiation, etc.) are affected in cells expressing TDP-43 fragments without the RRM-1 or glycine-rich domain or both.